Quaternary Science Reviews 334 (2024) 108709

Contents lists available at ScienceDirect

Quaternary Science Reviews

journal homepage: www.elsevier.com/locate/quascirev

The oldest fossil hominin from Italy: Reassessment of the femoral diaphysis from Venosa-Notarchirico in its Acheulean context☆

Ileana Micarelli [a,b,1], Simona Minozzi [c,1], Laura Rodriguez [d,e,1], Fabio di Vincenzo [f], Rebeca García-González [e], Valentina Giuffra [c], Robert R. Paine [a], José-Miguel Carretero [e,g], Gino Fornaciari [h], Marie-Hélène Moncel [i,**], Giorgio Manzi [a,*]

[a] Department of Environmental Biology, Sapienza University of Rome, Italy
[b] McDonald Institute for Archaeological Research, University of Cambridge, UK
[c] Division of Paleopathology, Department of Translational Research and New Technologies in Medicine and Surgery, University of Pisa, Italy
[d] Área de Antropología Física, Departamento de Biodiversidad y GestiónAmbiental, Universidad de León, Spain
[e] Laboratorio de Evolución Humana, Universidad de Burgos, Spain
[f] Natural History Museum – Anthropology and Ethnology, University of Florence, Italy
[g] Unidad Asociada de I+D+i al CSIC Vidrio y Materiales Del Patrimonio Cultural (VIMPAC), Spain
[h] Maria Luisa di Borbone Academy, Villa Borbone, Viareggio, Lucca, Italy
[i] UMR 7194-CNRS – Histoire Naturelle de l'Homme Préhistorique, Institut de Paléontologie Humaine, Museum National D'Histoire Naturelle, Paris, France

ARTICLE INFO

Handling Editor: Mira Matthews

Keywords:
Human evolution
Middle Pleistocene
Europe
3D morphology
Paleopathology
Bone micro-anatomy
Early Acheulean

ABSTRACT

Venosa-Notarchirico is a musealized Lower Paleolithic site in southern Italy (Basilicata), where a human femoral shaft was discovered in 1985. The fossil specimen can be evaluated in the new light of excavations started in 2016, which provide a more updated and extensive picture of the site, including the crucial Ar/Ar date of 661-614 ka for the human specimen. This makes the fossil diaphysis from Venosa-Notarchirico (Vn-H1) the oldest fossil hominin found so far in the Italian peninsula, associated with the earliest evidence of genuine Acheulean in Europe. In this paper, we report a comparative morphometric analysis of this femur, as well as a paleopathological reappraisal of the periosteal alteration that affects the specimen, supported by an unpublished histological analysis. Vn-H1 represents the proximal two-thirds of a right femur lacking the epiphyseal region. We argue it belonged to an immature individual, possibly a juvenile (late adolescent). Its features suggest that the specimen may refer to an archaic (*i.e.*, non-modern) human species, also showing morphological differences compared to fossil samples of the Neanderthal lineage. We also support the identification of a pathological condition affecting Vn-H1, particularly evident in some preserved portions of the mid-shaft as described here. Its etiology is discussed after differential diagnosis, which led us to suggest an alteration of inflammatory origin, viewed as a nonspecific periosteal response. This pathology may have been roughly concomitant with the death of the individual.

1. Introduction

The Paleolithic site of Notarchirico in the Venosa basin (Basilicata, southern Italy; Fig. 1) was discovered in 1979 and excavated for more than thirty years under the direction of the late Marcello Piperno (*e.g.*, Piperno, 1999). In 2016, new excavations started under the direction of one of us (MHM), with the aim of examining the stratigraphic levels underlying the hitherto known sequence. In this perspective, starting from layer F, dated to 670 thousand years BP (ka), there are four units dated by A40/A39 and ESR that are still under excavation (*i.e.*, layers G, H, I1 and I2), which include archaeological material (Pereira et al., 2015; Moncel et al., 2020, 2023).

☆ This work is dedicated to the memory of the late prof. Marcello Piperno, who passed away in February 2022 at the age of 76; he spent many years of his outstanding activity to the excavation, analysis and musealization of the prehistoric site of Venosa-Notarchirico.

* Corresponding author.
** Corresponding author.
E-mail addresses: marie-helene.moncel@mnhn.fr (M.-H. Moncel), giorgio.manzi@uniroma1.it (G. Manzi).

[1] Authors that contributed equally to this work: Ileana Micarelli, Simona Minozzi, Laura Rodriguez.

https://doi.org/10.1016/j.quascirev.2024.108709
Received 5 February 2024; Received in revised form 30 April 2024; Accepted 1 May 2024

The stratigraphic sequence of Notarchirico is now defined by a 7 m thick deposit of volcanic sediments derived from the Vulture Volcano's eruptions, whose layers are interposed with those documenting human presence in an ancient phase of the Middle Pleistocene. The stratigraphy of the site includes two marine isotope stages (MIS), the interglacial MIS 17 (from layers I2 to the base of layer F; see Fig. 1c) and the glacial event MIS 16 (from layer F to the top of the sequence) (Piperno, 1999; Moncel et al., 2020).

This time frame also corresponds to the maximum period of activity of the nearby volcano. The lithology and sediments of the whole sequence, referred to MIS 16 and MIS 17, are composed of volcano-derived and non-volcanic sands, crossing with layers of pebbles (Raynal et al., 1999; Lefèvre et al., 2010; Pereira et al., 2015). Fluvial processes governed this sedimentation, and volcaniclastics do not represent direct inputs, being in a secondary deposition. Some layers (α, A, B, C, F and I2) are lag deposits with a dense accumulation of cobbles and pebbles (referred to as "pavements").

From the Paleolithic record – spanning a period of almost 100.000 years – it is inferred that the site was occupied repeatedly, for short periods during interglacial and glacial events, between 614 ± 12 ka and 695 ± 6 ka (Pereira et al., 2015; Moncel et al., 2020), by Acheulean toolmakers. Thus, the basal level of the entire sequence (level I2) – yet showing evidence of human occupation – has been A40/A39 dated to a very early age for an Acheulean site in Europe (Moncel et al., 2020).

The documents of human occupation consist of lithic assemblages associated with faunal remains of various mammal species, including *Elephas antiquus* (Moncel et al., 2020). Regularly over the sequence, during about 100.000 years, hominins selected various calcarenite limestone pebbles to make bifaces and large cutting tools (LCTs) (Moncel et al., 2019, 2020; Santagata et al., 2020), as well as small nodules of chert for producing tiny flakes retouched by marginal or denticulated retouched on one edge or the entire perimeter (Moncel

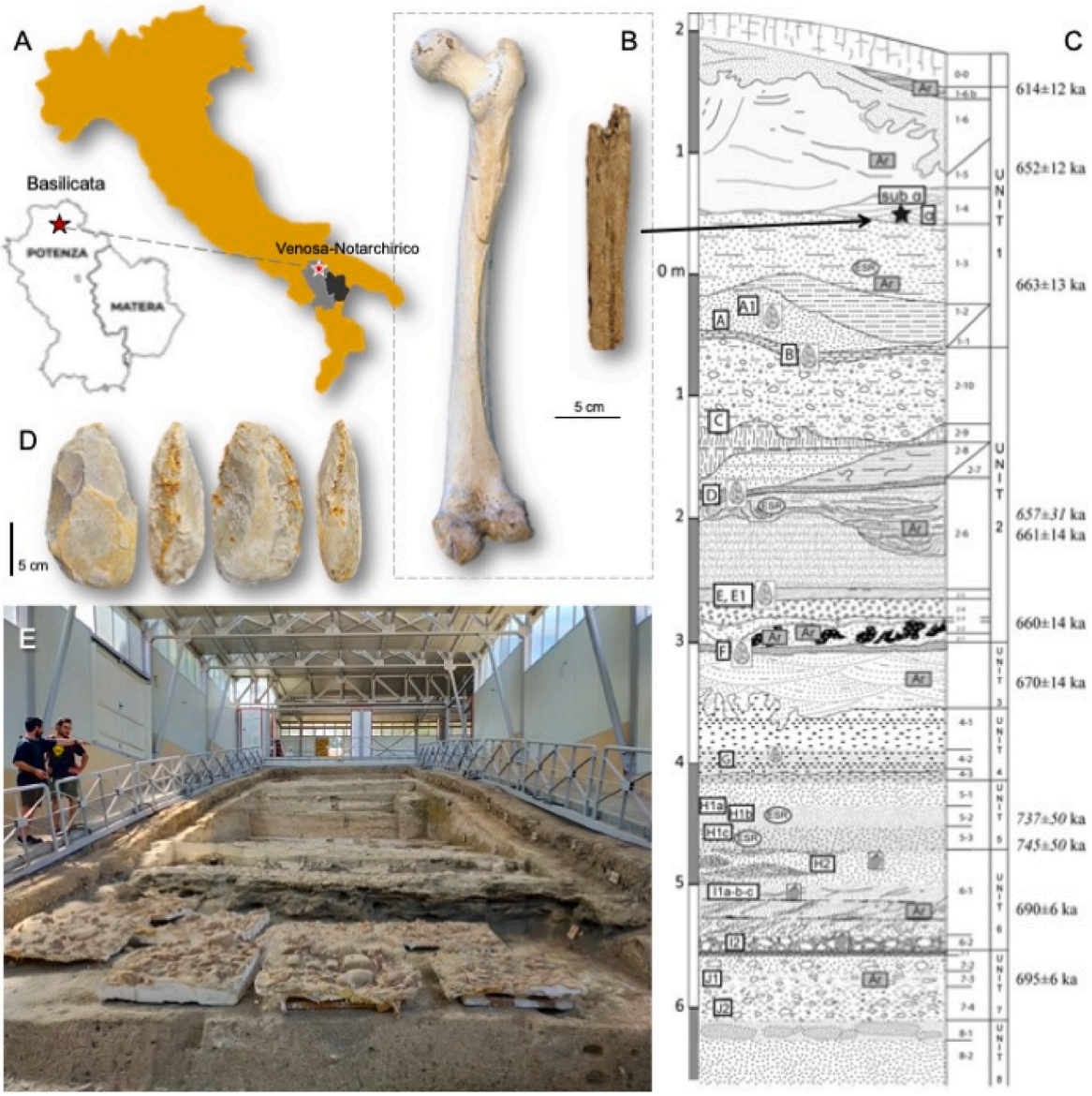

Fig. 1. Geographical location of Venosa Notarchirico in the northernmost Basilicata region, southern Italy (A). The femoral shaft Vn-H1 (shown in posterior view, B) was discovered in 1985 in the upper levels of the stratigraphy (level alpha of Unit 1, 1–4); it is compared here to a complete human femur from the Middle Pleistocene of Europe (F-XIII from At- SH) and inserted (C) in the stratigraphic sequence of the Notarchirico Paleolithic site (see legend in Moncel et al., 2023). In figure (D, E) there is also an example of the Acheulean handaxes that have been found (Moncel et al., 2023) and a recent image of the musealized site, viewed from its basal side (oriented north).

et al., 2023). The small tool component comprises small, retouched flakes, thick convergent retouched tools and becs. Small cubic nodules are also directly retouched by abrupt retouches. Bifaces and LCTs are present in only some layers, possibly depending on the extension of the excavated areas and/or the activities practised *in situ* and/or local cultural traditions (Rineau et al., 2022). Preliminary micro-wear analyses suggest, in some cases, domestic activities (Moncel et al., 2020). So far, no clear evidence of anthropic scavenging on animal carcasses has been recorded.

This site is unique within Europe in displaying, at the same time, a very early Acheulean lithic assemblage and several occupation phases, with or without handaxes. The systematically excavated 15 layers of Venosa-Notarchirico represent, at present, the most extended sequence of human occupation for this age, at least in Southern Italy, combined with the clear evidence of hominin occupations. In this regard, the absence of Acheulean sites in Western Eurasia before 700 ka must be underlined (Di Vincenzo and Manzi, 2023), with the single exception of the Spanish site of La Boella, dated to 900 ka, which has yielded some crudely-made handaxes due to either a local evolution or a punctual occurrence of an early Acheulean (Ollé et al., 2023; Vallverdú et al., 2014). Nonetheless, there are no other traces of *in situ* evolution or diffusion of bifacial assemblages in Europe until sites dated around 700 ka, where evidence of an Acheulean with symmetrical and full-volume bifaces is abruptly observed, one of the oldest and systematically excavated of these sites is Venosa-Notarchirico.

In this context, it was in 1985 that the shaft of a fossil human femur was discovered in the upper part of the volcanic layers (see Fig. 1; Piperno, 1999); it will be referred hereinafter to as Vn-H1. Initially, the specimen was attributed to an age of 500 ka. However, the new excavations and analyses at the site have dated the femur by Ar/Ar to an age bracketed between 661 and 614 ka (Pereira et al., 2015); thus, Vn-H1 the oldest hominin fossil found so far within the Italian peninsula (*e.g.*, Buzi et al., 2021) and among the oldest after MIS 18-16 in Europe (Di Vincenzo and Manzi, 2023; Hu et al., 2023).

A previous study of the bone assigned the femur to an adult female, with morphological affinities to *Homo erectus* (Belli et al., 1991). This *taxon*, however, has never been recognized in Europe at least so far. Therefore, given the renewed interest in the human femoral shaft from Venosa-Notarchirico, we decided that a reappraisal of its features was required. Our study, therefore, includes a detailed comparative morphometric study and a histological analysis of the specimen. The latter, in particular, is aimed to determine univocally the etiology of the pathological alteration that occurred to the diaphysis of this femur.

2. Material and methods

The human specimen from Venosa-Notarchirico (Vn-H1, Fig. 2) consists of a large fragment approximately 20 cm long of a right femoral shaft, extended roughly between the subtrochanteric (surgical neck) level and a portion distal to the mid-shaft. It includes approximately 85%–35% of the standard levels defined by Ruff and Hayes (1983). The proximal and the distal fractures are irregular (Fig. 2c). A small fragment from the distal region of the femur was removed for histological assessment in the late 1980s (Belli et al., 1991). The thin sections are no longer available for reassessment, while photos of these cross-sections have been recovered and are available for investigation (see Figs. 6–8). As Fig. 5d shows, only the region with the periosteal lesion was sectioned for histological evaluation.

2.1. Comparative samples

For morphological and metrical comparisons, we use data about the Pleistocene fossil record derived from both original specimens collected by the authors and from the literature. Our comparative sample includes data from the original specimens from the European Lower Pleistocene site of Gran Dolina (TD-6 level) (Carretero et al., 1999), dated 800–900 ka (Moreno et al., 2015), and from the Middle Pleistocene site of Sima de Los Huesos (At-SH), dated 430 ka, (Arsuaga et al., 2014, 2015), both in the Sierra de Atapuerca. The sample from At-SH includes adults and non-adult individuals, overall juvenile (*i.e.*, adolescent) individuals (Rodríguez et al., 2018; García-González et al., 2016). In At-SH site, over 7000 human fossils have been recovered, representing at least 29

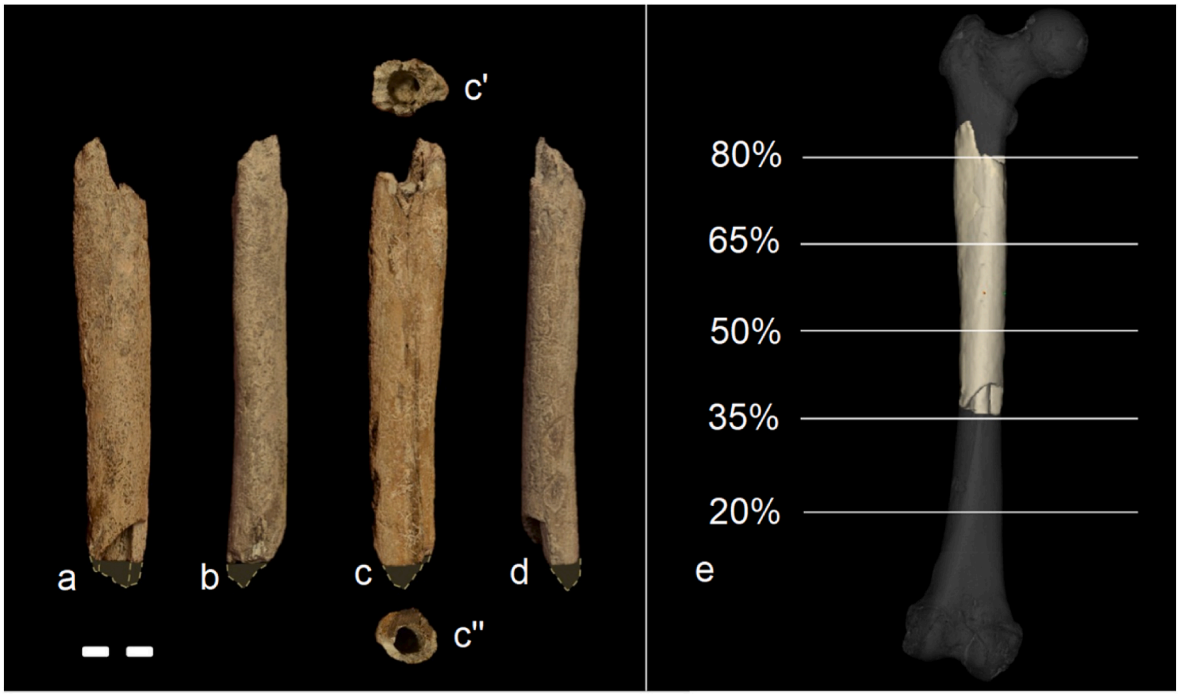

Fig. 2. The femur from Venosa-Notarchirico (Vn-H1), various views of the shaft: a) anterior; b) lateral; c) posterior, c') proximal, c") distal (after the histological sampling); d) medial. The distal fragment shaded in grey (defined by a dotted line) was removed in the late '80s for histological analyses. In (e), the specimen is anatomically placed between approximately 35% (distally) and 85% of an adult human femur.

individuals based on dental remains, with the majority being adolescents or young adults (Arsuaga et al., 2015; Bermúdez de Castro et al., 2021). Although, up to now, there has been no association between adolescent dental individuals and those represented by femora, the age distribution based on non-adult femoral remains is entirely consistent with that obtained from dental remains of non-adult individuals (García-González et al., 2016). Furthermore, the state of fusion of most of the SH non-adult femora clearly indicates that they are in the adolescent period. Thus, the most plausible scenario is that these femora belong to these dental individuals. Thus, the sample from At-SH includes adults and those belonging to adolescent individuals (Rodríguez et al., 2018; García-González et al., 2016). The information on other European, Asian and African Pleistocene femora is derived from the literature (Table 2). For the diaphyseal cross-section analysis, besides the original fossils from At-SH, we have also measured a sample of recent femora of adult and adolescent individuals from the Medieval archaeological sample of San Pablo Monastery (SPM, Burgos), housed in the Laboratorio de Evolución Humana at the University of Burgos (García-González et al., 2024).

2.2. Cross-sectional geometric properties

The cross-sectional shape and thickness of the bones reflect their robustness and rigidity in different planes and axes. To perform this analysis, a series of cross-sectional parameters were measured on Vn-H1 as well as in the At-SH and the recent SPM samples, following Ruff et al. (1993): total subperiosteal area (TA); cortical subperiosteal area (CA; a measure of resistance to axial loads); maximum (Imax) and minimum (Imin) second moments of area (to assess bending rigidity in the reference planes); polar second moment of area (J; an indication of resistance to torsion and overall rigidity) and section moduli at bone mid-shaft (Z; to measure bending and torsional strength and where Zp represents the cross-sectional torsional strength). Cross-sections parameters – at the 80%, 65% and 50% levels of biomechanical length – were obtained using Moment-Macro for ImageJ following Ruff and Hayes (1983) and Trinkaus and Ruff (2012); see https://www.hopkinsmedicine.org/fae/mmacro.html.

Since Vn-H1 is filled with cemented sediment and is also affected by pathological bone apposition in the periosteum (see below), a CT scan was performed to isolate its cortical shell virtually. Tomographic scanning of the Vn-H1 femur was carried out at Casa di Cura PIO XI (Rome, Italy), using a GE medical systems/revolution CT scanner with an energy of 100 kV and 250 mAs, an image size of 512 x 512 pixels, a slice thickness of 1.250 mm, and a pixel size of 0.625 mm. For comparison, CT-scans of the Middle Pleistocene At-SH and recent SPM samples were performed at the University of Burgos (Spain), using a YXLON Compact X-Ray industrial multi-slice computed-tomography scanner, with an energy of 160 kV and 4 μA, a collimated slice thickness of 0.5 mm and an inter-slice spacing of 0.3 mm. The CT images were obtained as a 1024 x 1024 matrix of 32-bit Float format with a pixel size of 95 μm, and visualized using the software package Mimics 21.0v (Materialise, 2009). The digital mesh of Vn-H1 is available upon request.

To highlight the mid-shaft cortical distribution pattern of Vn-H1, we performed a mapping of bone cortical thickness with BoneJ Plugin implemented in ImageJ (Hildebrand and Rüegsegger, 1997; Dougherty and Kunzelman, 2007). This mapping was also used for the Arago lower limb bones by Chevalier and Lumley (2022a,b). As a rule, a pathological external bone in the CT images can be identified as a lower-density bone in the outer perimeter, and usually can be easily distinguished from both the outer border effect and the cortical limit. At the original distal fracture level of Vn-H1, the pathologic bone is visible and easier to see with the naked eye (Fig. 5d). On the contrary, at the 80%, 65%, and 50% shaft levels, the altered pathological surface is very thin, and its low-density signal in the CT images is very weak. We believe that the pathology does not alter the original external or internal cross-sectional shape at these levels, and the cross-sectional parameters can be calculated with confidence.

2.3. Age at death of Vn-H1

The age at death of isolated bones of fossil specimens is difficult to assess; as a matter of fact, in most cases just the mature or immature status is indicated. Nevertheless, as histomorphometric, cross-sectional geometric and gross morphological traits change with age, even the mature or immature status could be important for accurate comparative purposes.

Although it is almost impossible to make a firm decision based on external dimensions, the growth trajectory of cross-sectional parameters can help us in concluding a general age estimation for Vn-H1. Growth-related changes in size and shape of femoral cross-sections have been extensively studied. This enquiry has shown that during infancy and childhood there is a net gain of cortical bone, mostly influenced by changes in mechanical loadings caused by locomotor development (Cowgill, 2010; Gosman et al., 2013; Swan et al., 2020). During adolescence, the effect of steroid lead to cortical bone being added at both surfaces in both sexes, which could result in a medullary contraction (Frisancho et al., 1970; Garn, 1970; Chevalley et al., 2009). We have compared the mentioned cross-section parameters in fossil and recent specimens in order to investigate the possible age at death of Vn-H1.

At this moment only, photos of femoral micro-anatomy are available for assessment (see Fig.. 5c and 6a-c, 7a,b), still we can provide subjective assessment of the micro-anatomical features. This kind of observations provides an idea of the extent of both the modeling (woven bone production) and remodeling (secondary osteons formation) processes occurred to this specimen. These micro-anatomical features are useful in assessing a general age-at-death estimation (sub-adult or adult) and the state of lesion formation. To complete an attempt to describe the histological nature of the femoral cross-section, we determined if the following features are present or absent (Table 1). These are typical features used in histological evaluations to determine the general state of dry bone remodeling and modeling in long bones.

2.4. Paleopathological investigation

A previous description of Vn-H1 (Belli et al., 1991) highlighted the occurrence of bone neoformation localized on some portions of the diaphysis, diagnosed as periostitis and attributed the bone apposition to infection, perhaps caused by an injury to the thigh. In such a framework, a small fragment of the distal end of the bone (see Fig. 2) was removed in the late 1980s to obtain thin slices for histological examinations; the relevant images of this preparation (see various figures further on) had not published, but have fortunately been preserved in the laboratory of one of us (GF). The original slides have now been carefully re-examined under a 100-400x light microscope and a comprehensive photographic documentation has been obtained.

Table 1
Histological features and cortical bone regions.

Histological feature	References
Primary osteons	McFarlin et al. (2016)
Intact secondary osteons N. On	Frost (1985), Parfitt et al. (1987), Stout and Paine (1992)
Fragmentary secondary osteons N. On. Fg.	Frost (1985), Parfitt et al. (1987), Stout and Paine (1992)
Howship's Lacuna	Robling and Stout (1999)
Double zonal osteon	Robling and Stout (1999), Gocha et al. (2018)
Drifting osteon	Robling and Stout (1999), Gocha et al. (2018)
Banded osteon	McFarlin et al. (2016)
Woven bone	McFarlin et al. (2016)
Primary lamellar bone	McFarlin et al. (2016)
Periosteal envelope	Frost (1985)
Haversian envelope	Frost (1985)
Cortical-Endosteal envelope	Frost (1985)

In order to evaluate the pathology through macroscopic observations and histology, we thus performed a new examination of the femur, combining this observation with the analysis of the micro-anatomical features visible on the preserved histological images of the small fragment sampled after the discovery (Belli et al., 1991). A new description of the outer cortical shaft surface and a discussion of both the micro-anatomy and the histological features of the cortical bone are reported here, while a review of the paleopathological literature for a differential diagnosis of this bone formation is also discussed. In doing so, we rely on the work of Weston (2012), who refutes some of the findings (specific histology features used to diagnose lesion origins in bone) by Schultz (2001).

3. Results

3.1. Gross anatomy, cross sectional morphometrics and micro-anatomical frequencies

Proximally, the posterior surface is characterized by a deep gluteal (hypotrochanteric) fossa and laterally by a blunt and well projected lateral crest, which taken together produce a marked antero-posterior (AP) flattening of the proximal shaft (platymeric femur), as evidenced also by the compressed AP cross-section at this level (Fig. 3). The absence of true pilaster stands out on the posterior surface, and the distal cross-section is almost subcircular, showing thick cortical walls. In the preserved portion, there is no signal of antero-posterior curvature of the shaft. In most of these traits Vn-H1 resembles other archaic femora, with reference to the human fossil record which is bracketed between the Early Pleistocene and the emergence of *Homo sapiens*.

In Table 2 and Fig. 4, we give the basic external dimensions of Vn-H1 compared with other Middle and Upper Pleistocene fossil femora, and in Table 3, the cross-sectional parameters of Vn-H1 at the three different levels.

In absolute dimensions, Vn-H1 is one of the smallest femora of all the fossil specimens used for comparison in this work, either when we consider diameters or perimeters at mid-shaft or at the subtrochanteric level. For example, only four of the femora in our comparative sample (Table 2) have the mid-shaft perimeter below 85 mm as Vn-H1: namely, the Tabun C1 adult Neanderthal woman, the late adolescent F-XVI from At-SH and the Pekin II and V specimens whose age remain unknown (Ruff et al., 2015). Moreover, in its general external dimensions, Vn-H1 is in the line of the late adolescents F-IV, F–V and F-XV from At-SH.

As shown in Fig. 3, the At-SH femurs lack a proper pilaster and, in possible association with this trait, show a medial cortical thickening at mid-shaft (medial buttres in Rodríguez et al., 2018), which is also frequent in other archaic femora (Trinkaus and Ruff, 2012; Chevalier and Lumley, 2022a), now including Vn-H1. Chevalier and Lumley (2022a) differentiate the pattern of cortical distribution at the femoral mid-shaft and along the femoral diaphysis in some Pleistocene hominins and, according to them; this pattern would be a good indicator of evolutionary affinities. The femoral cross-section at mid-shaft in Arago (A-141) displays roughly similar cortical bone thickness in each direction and this distribution is also present in the Zhoukoudian femora and KNMER 1808; Chevalier and Lumley (2022a). In contrast, the femurs from At-SH show postero-medial cortical reinforcement (*i.e.*, postero-medial bone cortical thickening at mid-shaft), a pattern that is frequent in Neanderthals and some (*e.g.*, Karain, Ehringsdorg), but not all (*e.g.*, Lazaret) European Pleistocene hominins. Moreover, the pattern of Trinil and Zhoukoudian femora is close to Arago and differs to At-SH and the Neanderthals (Chevalier and Lumley, 2022a).

The cortical bone distribution at mid-shaft of Vn-H1 is almost the same on all sides of the mid-shaft cross section (see Fig. 3) and it has a maximal thickness on the medial and lateral sides and the least cortical thickness value on the anterior side. Thus, for this trait Vn-H1 is like Zhoukoudian and Arago and different from the femora from At-SH and of the Neanderthals. Given the chronology of Vn-H1 (661-614 ka), this could be a relevant trait with phylogenetic meaning (*e.g.*, Manzi, 2016; Di Vincenzo and Manzi, 2023). Nevertheless, in our view, the developmental status of the fossil specimens used in the comparisons must be kept in mind.

The pattern of change of cortical distribution along the proximal femoral diaphysis (80%, 65%, 50%, 35%) can be also informative in this sense, and Chevalier and Lumley (2022a) detect what they call the spiral distribution pattern of diaphyseal maximal cortical thickness. This spiral originates on the proximal and medial diaphyseal region and ends approximately at mid-shaft on the postero-medial region. Thus, they differentiate the *Homo erectus*-like medial buttress, associated with straight medial reinforcement, to the Neanderthal and At-SH postero-medial buttress, associated with an oblique reinforcement (also called spiral reinforcement). The pattern of cortical distribution along the proximal region of Vn-H1 can be determined (at least) for the 80%, 65% and 50% levels (see Fig. 3). The comparison of Vn-H1 indicates that this specimen doesn't present the oblique or spiral buttress we see in At-SH and the Neanderthals but the straight medial reinforcement as in Zhoukoudian and Arago. It is very interesting to note that the late adolescent F-XVI from At-SH already shows the spiral buttress that can

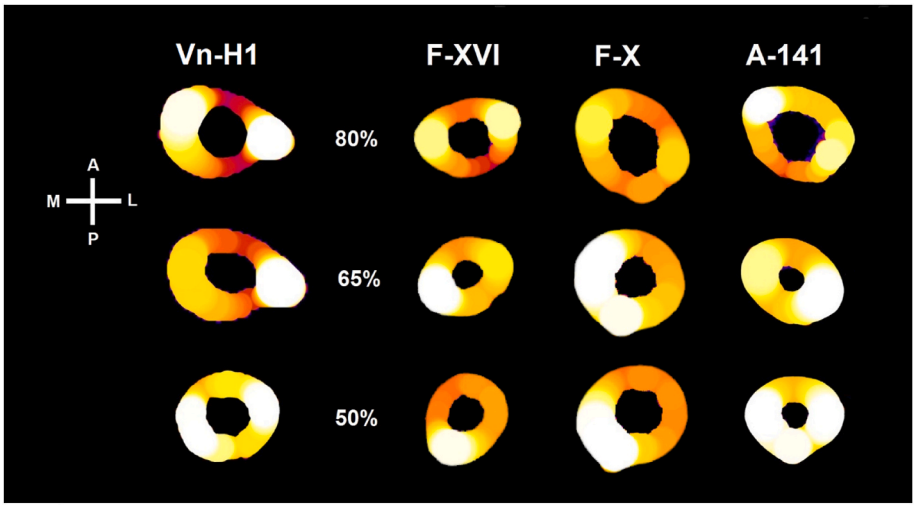

Fig. 3. Cross sections of Vn-H1 at approx. 80%, 65% and 50% compared with those of F-X and F-XVI from At-SH (Rodríguez et al., 2018) and Arago A-141 (Chevalier and Lumley, 2022a, 2022b). F-X and F-XVI are from the left side, while data from Vn-H1 and A-141 come from the right side. Sections are not size scaled, but are drawn approximately to the same size. *Legend*: white = greater thickness; red/purple = lower thickness.

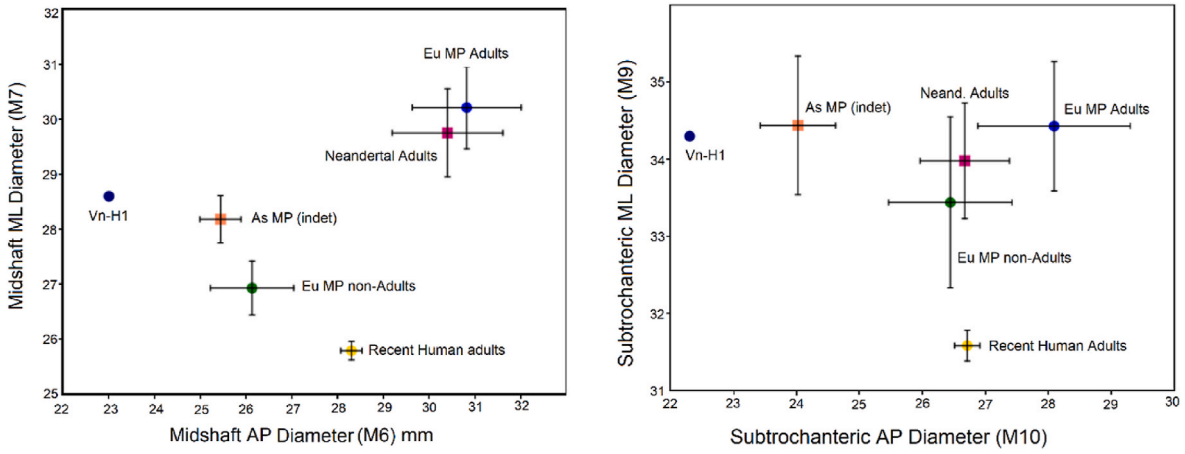

Fig. 4. Scatter plot of antero-posterior (M6) versus medio-lateral (M7) midshaft diameters (left) and antero-posterior (M10) versus medio-lateral (M9) subtrochanteric diameters (right) in fossil and recent samples. The means and standard error are represented. Eu MP = European Middle Pleistocene; As MP = Asian Middle Pleistocene. Composition of fossil samples and maturity stages as in Table 2. Recent human sample measured by the authors at the Museu e Laboratorio antropológico da Universidade de Coimbra (Portudal), n = 140.

be observed in the adult F-X of the same site.

3.2. Age at death of Vn-H1

Belli et al. (1991) assigned the Vn-H1 femur to an adult female based on its small size. However, looking at the large At-SH collection that include adult and subadult femora at different growth ages, we are more inclined to believe that Vn-H1 belonged to a subadult, namely to an adolescent individual.

In any case, Vn-H1 is a small specimen in comparison to the other fossil femora reported in Table 4; its external dimensions are at the lower limit of the fossil adult range, while it also fixes well among the adolescent individuals from Atapuerca At-SH. Regarding the internal parameters, at mid-shaft (50%) the TA and CA values of Vn-H1 fall within the range of variation observed for the recent SPM adults and adolescents. However, in comparison to At-SH adults, the TA is significantly lower, and the CA is towards the lower limit of their range of variation. As much as cross-sectional parameters can help, the value for Vn-H1 is lower than both At-SH and SPM adults and more in line with their respective adolescent samples. As for the relative cortical area (%CA), there are not statistically significant differences between adults and adolescents in the At-SH and SPM samples. However, the average %CA of the adolescents is higher than that of the adults in their respective groups, reflecting that they were still growing. Once more, Vn-H1has a %CA at mid-shaft is in line with the value of the At-SH adolescents and above the At-SH adults. Therefore, we consider the relevance that the dimensions of Vn-H1 for TA, CA, MA and %CA are very close to those observed in the At-SH adolescents.

Regarding the second moments of area (lx and ly) at mishaft, Vn-H1 exhibited a low antero-posterior second moment of area (Ix) compared to all age groups used in this study, while the mediolateral second moment of area (Iy) falls within the range of variation observed in At-SH adolescents and SPM adults. The same condition is observed for the maximum (Imax) and minimum (Imim) second moments of area, reflecting a diaphyseal shape more transversally oval. As a consequence, the indices Ix/Iy and Imax/Imin values for Vn-H1 are also low compared with the four age group samples (Tables 3 and 4).

As mentioned above, during adolescence the effect of steroid lead to internal and external cortical bone remodeling, which result in a medullary contraction (Frisancho et al., 1970; Garn, 1970; Chevalley et al., 2009). This explains why the %CA values of adolescents of At-SH and SPM are slightly higher than those of their respective adults. The At-SH and SPM seem to follow a similar pattern of change from adolescence to adulthood for TA, CA, MA and %CA. Neanderthals follow the same ontogenetic trend that At-SH and recent humans, but they exhibit larger cortices and total areas at all ages (Cowgill, 2010). Thus, the pattern exhibited by Vn-H1 is the one expected by an adolescent of an archaic human group, as can be demonstrated looking at the At-SH sample.

The main difference between Vn-H1 and the At-SH adolescents is related to the lower values of the former in the Ix, Imin and the ratios Ix/Iy and Imax/Imin, reflecting the more transversely oval mid-shaft shape. The histological analysis of Vn-H1 shows that there is new bone apposition on the periosteal surface, but with no pathological response observed on the endosteal surface. Consequently, both TA and CA values in Vn-H1 are those expected for the adolescents of an archaic population and below those observed, for example, in the At-SH and Neanderthal adults.

The adolescent age estimation for Vn-H1 is also supported by secondary osteon patterns (see Fig. 6). The ratio of the secondary intact osteons (N.On.) relative to fragmentary osteons numbers (N.On.Fg.) is high, giving a ratio of 14:1. This ratio indicates that there is a larger number of N.On. (56) relative to a smaller number for N.On.Fg. (4). This age estimation using osteons numbers is consistent with what has been observed in age estimating formulas used by forensic anthropologists (*e.g.*, Stout and Paine, 1992); typical N.On./N.On.Fg. for adults in their late twenties early thirties is 6:1 or 5:1, indicating a higher number of fragmentary osteons as age increases.

3.3. Paleopathological investigation

Macroscopic examination of Vn-H1 reveals postmortem damage of the cortical surface in the form of numerous minor serpiginous and irregular grooves, mostly (but not only) located on the medial and anterior sides of the diaphysis. The original cortical bone, also observable in post-mortem fractured areas, seems to consist of a regular compact bone.

At the same time, distally and medially (Fig. 5), the surface of the bone has a porotic appearance with thin longitudinal striations, confirming the presence of bone neoformation 1–2 mm thick, as reported in the previous study (Belli et al., 1991). The new pathological bone extends from the medial to the anterior surface of the distal portion of the diaphysis, while some minor residual areas of the same neoformation are also visible in other undamaged points. The sampling for histology of this pathological alteration was performed at a cross-section of the diaphysis in an area preserved from post-mortal damage. The trabecular appearance of the new bone apposition, clearly visible even to the naked eye (Fig. 5b–d), involves the external surface of the cortical bone.

An observation by light microscope (Fig.. 5c, 6 and 7, 8) clearly

Table 2
External dimensions (in mm) of Vn-H1 compared to other Pleistocene fossil femora.

	Side	Maturity	MID-SHAFT LEVEL (50%)				SUBTROCHANTERIC LEVEL (80%)				Source
			AP Diam.	ML Diam.	Circumference	Midshaft (pilastric) Index	AP Diam	ML Diam	Circumference	Platymeric Index	
			M6	M7	M8	M6/M7	M10	M9		M10/M9	
Middle Pleistocene Europeans											
Venosa 1 (Vn-H1)	r		23.0	28.6	81.5	80.7	22.3	34.3	93.0	64.9	This study
SH F-X	l	adult	34.4	34.7	105.0	99.3	32.4	37.0	108.5	87.6	Carretero et al. (2023)
SH F-XII	l	adult	32.6	29.7	96.0	109.8	31.0	35.5	102	87.3	Carretero et al. (2023)
SH F-XIII	r	adult	31.9	28.4	93.0	112.1	30.1	34.9	101	86.2	Carretero et al. (2023)
SH F-XIV	r	adult	31.6	29.1	104.0	108.6	30.2	35.7	101	84.6	Carretero et al. (2023)
SH F-XVI	l	adolescent	23.4	27.9	88.8	83.9	23.3	32.2	89.0	72.4	This study
SH F-IV	r	adolescent	26.1	27.5	85.0	94.9	26.4	35.2	99.0	75.0	This study
SH F–V	l	adolescent	28.3	26.9	85.0	105.2	25.5	33.7	98.0	75.7	This study
SH F-XV	r	adolescent	26.7	25.4	82.0	105.1	28.4	29.9	85.5	95.0	This study
Castel di Guido 1	r	adult	35.0	32.0	104	109.4	–	–		–	Mallegni et al. (1983); Belli et al. (1991)
Castel di Guido 2	l	adult?	24.8	31.1	89.0	80.0	21.0	29.8		70.5	Mallegni et al. (1983); Belli et al. (1991)
Sedia del Diavolo 1	r	indet	31.6	29.4	95.0	107.5	–	–		–	Belli et al. (1991)
Ponte Mammolo 1	r	indet	33.4	29.5	96.2	113.2	28.7	34.6		82.9	Belli et al. (1991)
Arago 48	r	adult	–	–	–	–	28.9	35.7	–	81.0	Chevalier and Lumley, 2022b
Arago 57	l	adolescent?	–	–	–	–	28.6	36.2	–	79.0	Chevalier and Lumley, 2022b
Arago 141	r	adult	28.1	31.8	84.5	88.0	29.8	37.8	–	79.0	Chevalier and Lumley, 2022b
Ehringsdorf 5	r	adult	33.5	32.0	103.0	104.6	29.0	34.5		84.0	Belli et al. (1991)
Middle Pleistocene Asian											
Gesher Benot Ya'aqov	r	Indet	22.1	24.6		90	19.8	28.8		68.7	Geraads and Tchernov (1983)
Trinil II	r	Indet	26.2	27.1	85.0	97.0	26.2	37.7		80.1	Belli et al. (1991); Ruff et al. (2015); Ruff et al. (2022)
Trinil III	l	Indet	25.4	27.7	85.0	91.7	24.2	32.2		75.2	Belli et al. (1991); Ruff et al. (2015); Ruff et al. (2022)
Trinil lV	r	Indet	25.7	28.4	87.0	90.5	23.8	33.7		70.6	Belli et al. (1991); Ruff et al. (2015); Ruff et al. (2022)
Trinil V	l	Indet	27.0	26.3	85.0	102.6	–	–		–	Belli et al. (1991); Ruff et al. (2015); Ruff et al. (2022)
Pékin I		indet	27.1	29.7	98.0	91.2	23.2	34.3		67.6	Belli et al. (1991)
Pékin II		indet	22.8	26.4	77.0	86.4	–	–		–	Belli et al. (1991)
Pékin IV		indet	25.0	29.3	85.0	85.3	22.7	34.3		66.2	Belli et al. (1991)
Pékin V		indet	23.7	29.5	83.0	80.3	–	–		–	Belli et al. (1991)
Pékin VI		indet	26.1	29.2	85.0	–	–	–		–	Belli et al. (1991)
Upper Pleistocene Europeans											
La Quina HV	l				90.0		26.0	33.5		77.6	Heim (1976); Mallegni et al. (1983)
La Ferrassie 1	r	adult	31.0	32.0	99.0	96.9	28.0	39.0		71.8	Heim (1976)
La Ferrassie 1	l		29.1	31.0		93.9					Heim (1976)
La Ferrassie 2	r	adult	26.5	30.0	90.0	98.3	24.0	34.5		69.6	Heim (1976)
La Ferrassie 2	l		28.1	28.6		98.3					Heim (1976)
Spy 2	r	adult	29.0	29.0	90.0	100.0	25.0	36.0		69.4	Heim (1976); Mallegni et al. (1983)
Spy 2	l		26.0	29.0	89.5	89.7	30.0	39.0		76.9	Heim (1976); Mallegni et al. (1983)
Hortus 34	l						25.6	31.0		82.6	Mallegni et al. (1983)

(*continued on next page*)

Table 2 (*continued*)

	Side	Maturity	MID-SHAFT LEVEL (50%)				SUBTROCHANTERIC LEVEL (80%)				Source
			AP Diam.	ML Diam.	Circumference	Midshaft (pilastric) Index	AP Diam	ML Diam	Circumference	Platymeric Index	
			M6	M7	M8	M6/M7	M10	M9		M10/M9	
Neanderthal 1	r	adult	31.5	28.2	92.5	111.7	29.3	33.4		87.7	Mallegni et al. (1983)
Neanderthal 1	l	adult	30.6	30.1	92.0	101.7	28.4	36.0		78.9	Heim (1976)
La Chapelle	r	adult	34.5	27.5	98.0	125.5	32.0	33.0		97.0	Heim (1976)
La Chapelle	l	adult	31.8	29.0		109.7					Heim (1976)
Fond-de-Fôret	l	adult	33.5	30.0		111.7	27.0	37.0		73.0	Mallegni et al. (1983)
Sants Croce Cave 1	r	adult	29.7	29.0	91.0	102.4	25.7	32.0		80.3	Mallegni et al. (1983)
Krapina 213	l	adult					26.1	36.4	100.0	71.7	Trinkaus (2016)
Krapina 214	l	adult					22.3	29.6	80.0	75.3	Trinkaus (2016)
Lazaret 13	l	adult					28.7	36.2		79.3	Chevalier and Lumley, 2018
Lazaret 15/17	l	adult	22.8	24.0		95.0	24.4	29.3		83.3	Chevalier and Lumley, 2018
Upper Pleistocene Asian											
Amud 1	r	adult	33.0	32.0	106.0	103.1	31.0	37.0		83.8	Mallegni et al. (1983)
Tabun C1(*)	r	adult	22.0	24.0	81.0	91.6					McCown and Keith (1939)
Tabun C1(*)	l	adult	23.2	27.0		85.9	23.2	30.5		76.1	McCown and Keith (1939)
Shanidar 1	r	adult	–	35.5	–	–	28.6	35.3		81.0	Trinkaus (1983)
Shanidar 4	r	adult	35.5	31.1	102.0	114.1					Trinkaus (1983)
Shanidar 5	r	adult	36.5	33.2	108.0	109.9					Trinkaus (1983)
Shanidar 6	r	adult	28.5	28.0	89.0	101.8					Trinkaus (1983)

M# refers to the Martin and Saller (1957) variable number. SH = Sima de los Huesos.
(*) Although the taxonomic attribution of Tabun C1 fossil has been discussed (Tillier, 2005; Hershkovitz et al., 2021), it is included here among the Asian Neanderthals.

Table 3
Cross-sectional parameters of Vn-H1 femur at 50%, 65%, and 80% length levels.

	VN-H1	50%	65%	80%
Geometrical properties	TA	455	521	550
	CA	373	433	414
	MA	82	88	136
	%CA	82	83	75
	Ix	12698	13960	16302
	Iy	20000	33609	33566
	Imax	20005	33977	33923
	Imin	12693	13592	15946
	Zx	1147	1265	1343
	Zy	1398	1896	1892
	J	32698	47569	49869
	Zp	2260	2624	2788

Total area (TA) and Cortical area (CA) in mm^2. Moments of inertia Ix, Iy, Imax and Imin and J in mm^4. Section moduli Zx, Zy and Zp in mm^3. All values have been adjusted to zero decimal places.

shows the histological aspect of the lesion, revealing that the periosteal bone formation consists of an outer layer of relatively long and thin radiating trabeculae of woven bone, mainly in parallel orientation (Fig. 6). Large oval and round spaces (diameter 50–250 μm) occupy the external third of cortical bone; in some cases, an enlargement of the Haversian canals is present (Fig. 7). From Fig. 7 we also observe only one branching secondary osteon, 2 Howships lacunae, no double zonal osteons and, no drifting osteons. Additionally, no banded osteons are observed. The disorganized lamellar bone immediately below the periosteal envelope is the result of the periosteal growth of the surface lesion, while the Haversian systems assume an almost regular aspect in the central portion of the compact bone (Fig. 8); apart from some rare and scattered enlargements of the Haversian canals (Fig. 8d and e), the endosteum lacks any pathologic response. The micro-anatomical pattern mid-cortical to endosteal envelope appears lacking an affect by the lesion causing agent.

4. Discussion

4.1. General remarks

According to our results, following in part a previous study on Vn-H1 (Belli et al., 1991), the human diaphysis from Venosa-Notarchirico represents the proximal two thirds of a right femur lacking the entire epiphyseal region (the neck and head) of the bone. It most probably belonged to an immature individual, possibly a late adolescent, of an archaic (*i.e.*, non-modern) human species, more probably belonging to the controversial *taxon Homo heidelbergensis* (Shoetensack, 1908), whose holotype is only slightly younger than Vn-H1 (Wagner et al., 2010). At the same time, Vn-H1 shows morphological differences from specimens referred to the Neanderthal lineage (*i.e.*, the At-SH sample and the European and Asian Neanderthals). In view of the young age of the individual, the femur is of uncertain sexual attribution.

Its chronology is of utmost interest, since Vn-H1 has been dated between 661 and 614 ka (Pereira et al., 2015). Therefore, this shaft of a long bone represents the oldest fossil specimen ever found so far in the Italian peninsula (Manzi et al., 2010; Buzi et al., 2021) and among the oldest ones from the Middle Pleistocene of Europe (Di Vincenzo and Manzi, 2023). In addition, it is associated with a rich Paleolithic assemblage and faunal remains including various mammal species (Moncel et al., 2020).

The stratigraphy of Venosa-Notarchirico and the archaeological studies performed on the site (*e.g.*, Piperno, 1999; Moncel et al., 2020) suggest that it was occupied repeatedly for short periods of time during interglacial and glacial stages, between 695.2 ± 6.2 and 614 ± 4 ka (Pereira et al., 2015), that is between the interglacial MIS 17 and the glacial event of MIS 16, spanning a period of almost 100.000 years. Therefore, like the human femur, the Acheulean assemblage recorded at Venosa-Notarchirico, with or without the occurrence of handaxes, represents at present the oldest most extended sequence of this kind in Europe at the beginning of the Middle Pleistocene.

Table 4
Comparison of cross-sectional properties at midshaft (50%) of the femur in Vn-H1, At-SH and modern humans.

	Vn-H1	Sima de los Huesos		San Pablo	
		Adolescents	Adults	Adolescents	Adults
TA	455	435 ± 85	700.5 ± 134	312 ± 112.5	502 ± 92
CA	373	362 ± 74	556.5 ± 101.5	252 ± 115	375 ± 67
MA	82	72.5 ± 22.5	144 ± 33	60 ± 21	126 ± 40
%CA	82	83 ± 4	79.5 ± 3	78 ± 10	75 ± 5.5
Ix	12698	14800 ± 6760	45363 ± 12670	7980 ± 6285.5	19856 ± 7346
Iy	20000	15351 ± 5480	42889 ± 14669	6898 ± 5012	19764 ± 7849
Ix/Iy	0.63	0.8–1.1	0.9–1.2	1.0–1.2	0.7–1.5
Imax	20005	16179 ± 6900	50298 ± 16339	8077 ± 6347	218332 ± 8537
Imin	12693	13972 ± 5365	37954 ± 9975	6801 ± 4954	17714.5 ± 6519
Imax/Imin	1.6	1.1–1.2	1.2–1.5	1.0–1.2	1.0–1.6
Zx	1147	1202 + 422	2575 ± 586	769 + 441	1337.5 ± 319.5
Zy	1398	1285 + 266	2622 ± 670	598 + 269	1432 ± 387
J	32698	30151 ± 12227	88252 ± 26067	148787 ± 11294	39547 ± 14828
Zp	2260	2345 + 682	4991 ± 1287	1284 + 614	2646 ± 654

Variable mean and standard deviation except for the Ix/Iy and Imax/Imin in which the range of variation is given. TA (Total area), CA (Cortical area) and MA (Medullar area) are measured in mm2. %CA (relative cortical area) is computed as CA/TA*100. Ix and Iy (anteroposterior and mediolateral second moments of area) are measured in mm4. Imax and Imin (maximum and minimum second moments of area) are measured in mm4. Zx, Zy and Zp (section moduli) are measured in mm3. J (polar moment of area) are measured in mm4. All values have been adjusted to zero decimal places.

Furthermore, our work supports the identification of a pathological condition affecting Vn-H1, particularly evident in some preserved portions of the mid-shaft. This pathology may have been concomitant with the death of the individual, although it can be argued that he/she survived for some time after the infection involved the bony tissue. In the following paragraph we will discuss the possible etiology of this condition, through a procedure of differential diagnosis.

4.2. Morphology and morphometrics

Some morphological traits that are present in Vn-H1 can be considered plesiomorphic traits shared by all archaic humans since the Early Pleistocene, until the emergence of *Homo sapiens*. These femoral features are the following: large hypotrochanteric fossa, pronounced lateral crest, platymeric proximal section, lack of pilaster, subcircular mid-shaft cross-sectional shape and thick cortices.

Thus, these features are part of a complex of traits shared by archaic members of the genus Homo and have been reported for Early Pleistocene femurs from Europe, i.e. in the Atapuerca Gran Dolina sample (Carretero et al., 1999), from Asia (Weidenreich, 1941; Ruff et al., 2015) and from Africa (Day, 1971; Kennedy, 1983; Aiello and Dean, 1990; Gilbert, 2008), as well as for European Middle Pleistocene humans (Lumley and Lamy, 1982; Mallegni et al., 1983, 1987; Belli et al., 1991; Arsuaga et al., 1992; Rodriguez, 2013; Arsuaga et al., 2015) and Late Pleistocene Neanderthals (*e.g.*,McCown and Keith, 1939; Trinkaus, 1983; Ruff et al., 1993; Trinkaus and Ruff, 1999; Trinkaus et al., 1998; Puymerail et al., 2012). In modern humans (*i.e.*, *Homo sapiens*), the frequency of hypotrochanteric fossa varies (Aiello and Dean, 1990), but it is almost constant in archaic specimens.

A platymeric femoral diaphysis at 80% has been related to a body shape with a broad pelvis (Trinkaus and Ruff, 1999; Trinkaus et al., 1998). This is the case in At-SH hominins (Rodriguez, 2013; Arsuaga et al., 2015; Rodríguez et al., 2018), where this feature has been considered as part of the primitive biotype of the body *bauplan*, stocky and wide, that characterizes all archaic (*i.e.*, non-modern) *Homo* representatives, which changed and became derived only with the emergence of *Homo sapiens* (Arsuaga et al., 2015).

The histological study of Vn-H1 shows that there is new bone apposition on the periosteal surface, with no pathological response observed on the endosteal surface. However, despite this new bone formation, CSG parameters of Vn-H1 are lower than those observed in At-SH adults, while the same are expected for an adolescent of an archaic population.

Nevertheless, the pattern of cortical bone distribution along the proximal region of the diaphysis (*sensu* Chevalier and Lumley, 2022a) of Vn-H1 is in common with Zhoukoudian and Arago, whereas it is different from the femora of At-SH and the Neanderthals. Given the chronology of Vn-H1 (661-614 ka) this is a relevant trait of this specimen since it has been proposed as a good indicator of evolutionary affinities among the archaic hominins (Chevalier and Lumley, 2022a, 2022b). Here we must note that the late adolescent F-XVI from At-SH already shows the spiral buttress that can be observed in the adult F-X of the same site (see Fig. 3), which strengthens the idea of co-existence of different human lineages during part of the Middle Pleistocene (Manzi, 2011, 2016; Di Vincenzo and Manzi, 2023).

4.3. Paleopathology

The paleopathological alteration observed in the femur Vn-H1 is consistent with new bone apposition on the cortical surface, affecting most undamaged bone. The presence of small residual areas of new bone along the diaphysis suggests that taphonomic abrasion of the outer cortical surface might have removed the new apposition so that the initial assessment might have been thicker and wider in some parts of the shaft surface.

Bone has a limited response to injury or disease that stimulates the formation of bony defects or neoformation. In some cases, osteoblastic response to pathogens will produce new bone growth. In other instances, osteoclastic activity will lead to bone resorption. Occasionally, these agents will have bony growth defects and lytic lesions on the same surface (Burr and Allen, 2014). In the case of Vn-H1, the gross surface clearly shows a significant periosteal reaction producing new bone apposition. Histological analysis shows an apparent disturbance of a normal bone formation of the cortical bone, resulting in alteration of the periosteal envelope, woven bone production, and hypervascularization.

Several diagnostically defined agents might account for the observed defective changes in the femoral shaft, and a differential diagnosis is challenging to establish. Schultz (2001) grouped the periosteal alterations as inflammatory (periostitis) or noninflammatory processes (periostosis). The inflammatory processes include osteitis, osteomyelitis, and inflammation of the deep veins; non-inflammatory diseases are primary and secondary bone tumors, healing of bones after fracturing, hypertrophic osteoarthropathy, and other conditions. Recently, Roberts (2019: 288) reports: “periostitis should only be used to refer to inflammation due to infection, and it is well known that there are many causes of new bone formation beyond infection. […] Periostosis usually represents part of, or a reaction to, pathological changes of the underlying bone”.

The periosteal reaction observed in Vn-H1 might be due to several different pathological conditions that secondary affect the periosteum or can be due to a primary affection of the bone, such as traumas and infections. Observation is limited to a single incomplete bone fragment, and the monotonal response of bone tissue complicates the identification of its etiology. Although the correlation between histological manifestations and specific disease processes is a discussed argument (Weston, 2009, 2012), paleo-histopathological investigation can help to

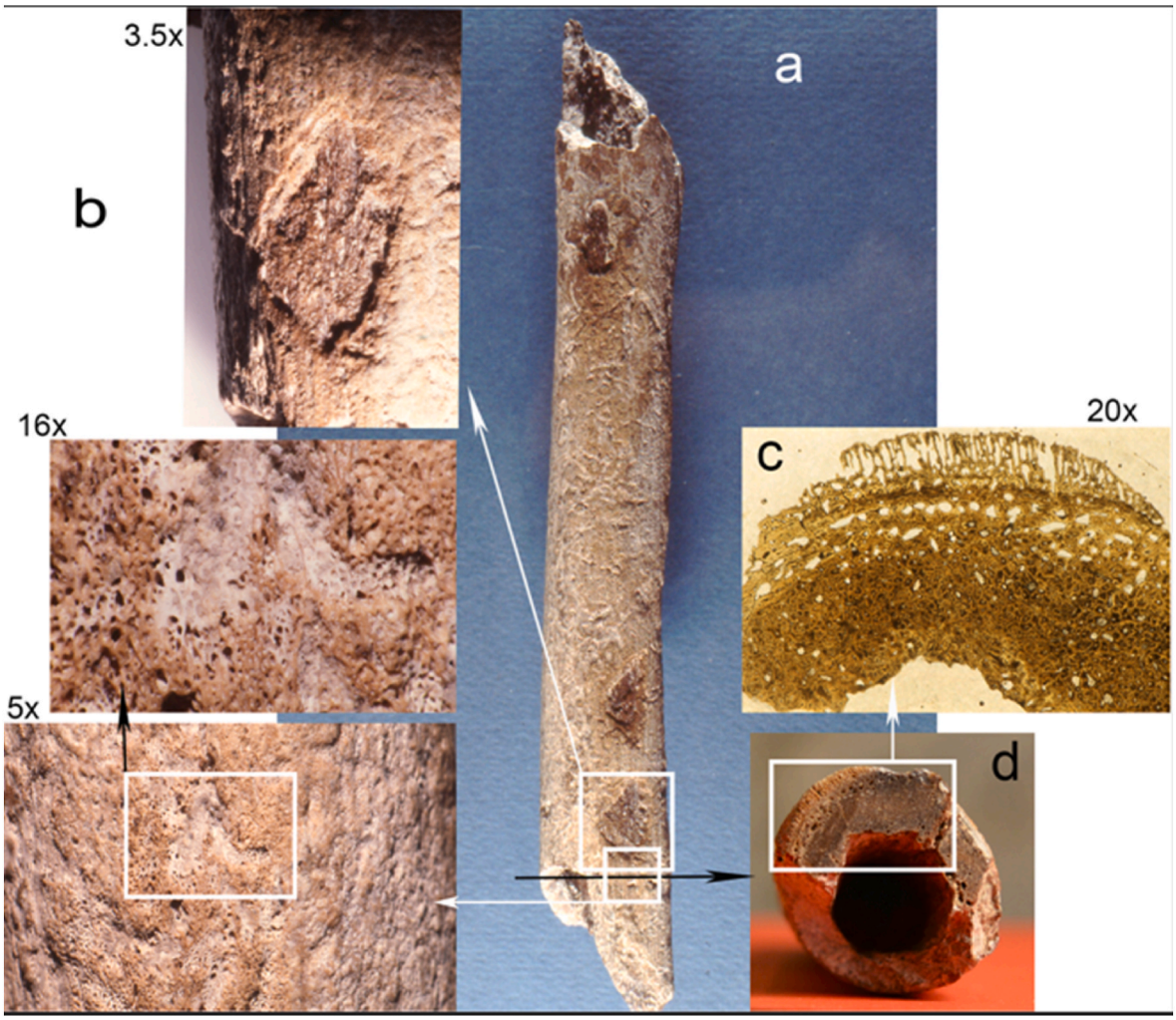

Fig. 5. Post mortem and pathological alterations observed in Vn-H1 and sampling: a) medial view of the shaft (from a photo taken after the discovery, when the sample for histology had not yet been removed); b) different magnifications of the affected surface (3.5×, 16x and 5x); c) histological cross-section of the affected cortical bone (20x); d) distal view of the shaft sampled for histology in the late '80s of the last century.

develop an appropriate differential diagnosis model to argue from. Several diagnostically defined agents might account for the observed bone changes in Vn-H1 femur. Lesions associated with the evidence on Vn-H1 femur are reported from the literature and discussed below.

4.3.1. *Circulatory disorders*

Vascular disorders, such as venous stasis in the lower limbs, may exert pressure on the bone surface, leading to inflammatory processes and stimulating new periosteal bone formation. Microscopically, short, and bulky trabeculae are developed, and multiple layers at the original bone surface can be produced (Grauer, 2019). This pathological condition can likely be associated with the Vn-H1 bone lesions. However, the paleopathological record for circulatory disorders is not spread to the whole diaphysis but limited to a limited area. Therefore, it is not possible to offer a comprehensive comparison with our specimen.

4.3.2. *Hematogenous osteomyelitis*

This pathology is due to a bacterial infection that spreads through the blood affecting the bone and marrow. The immunological response induces a remodeling process that involves both osteoblastic and osteoclastic activity, with new bone growth associated with the progressive development of an *involucrum*. The osteoclastic activity results in bone necrosis or *sequestrum* with cloacae for pus draining (Ortner, 2003; Waldron, 2009; Roberts, 2019). Osteomyelitis can also represent a secondary infection associated with compound fractures and/or external trauma (Aufderheide and Rodríguez-Martin, 1998). Osteomyelitis can be excluded since there is no cloacae present, *sequestrum*, *involucrum* and there are no changes in the mid cortical to endosteal envelopes of the cross section.

4.3.3. *Malignant tumors*

Cancer can often be directly traced to bone origin, such as osteosarcoma. Cancer can also be spread from soft tissues to bone through metastatic processes, causing osteolytic bone lesions. Such lesions can be either osteoblastic or osteoclastic in formation, sometimes both processes are observed. Osteosarcoma, prostate, and breast cancer can generally produce an osteoblastic response. The bone neoformation that involves the periosteum is usually aggressive. For example, in osteosarcoma, differently from Vn-H1, the massive "sunburst" (periosteal spicules arranged perpendicularly to the bone surface) or periosteal neoproduction is the most frequent picture (Marques, 2019). In advanced stages, the deeper structures of the original bone substance can be involved. Microscopically, the trabeculae show a more normal development (Schultz, 2001; Rana et al., 2009).

4.3.4. *Treponemal diseases*

Treponematosis is a bacterial infection which can affect bone, inducing a periosteal reaction with extensive woven-bone formation. In

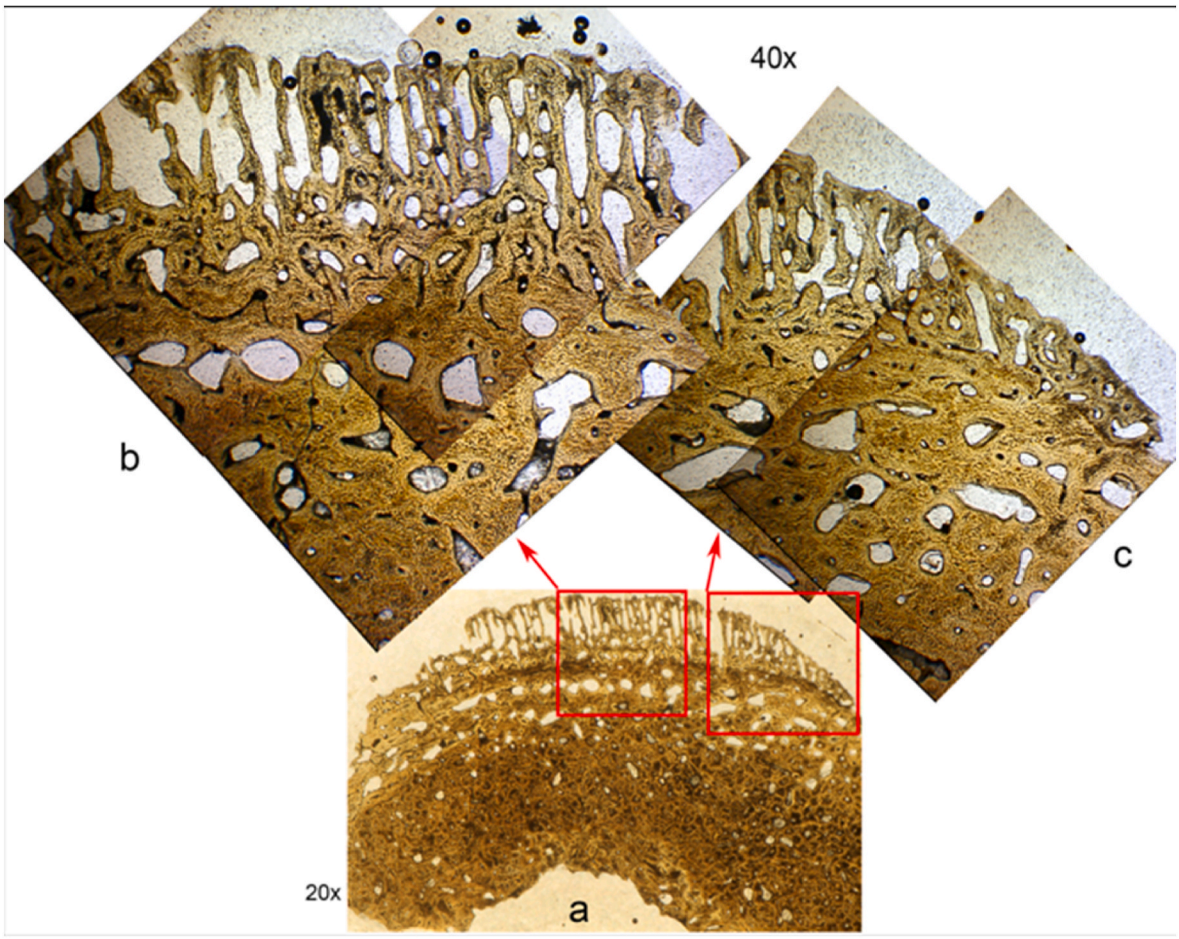

Fig. 6. Undecalcified ground cross section of the diaphysis: a) original compact bone of the shaft with bone neoformation, consisting in thin radiating trabeculae of woven bone (20x); b, c) photo are at 40× magnification.

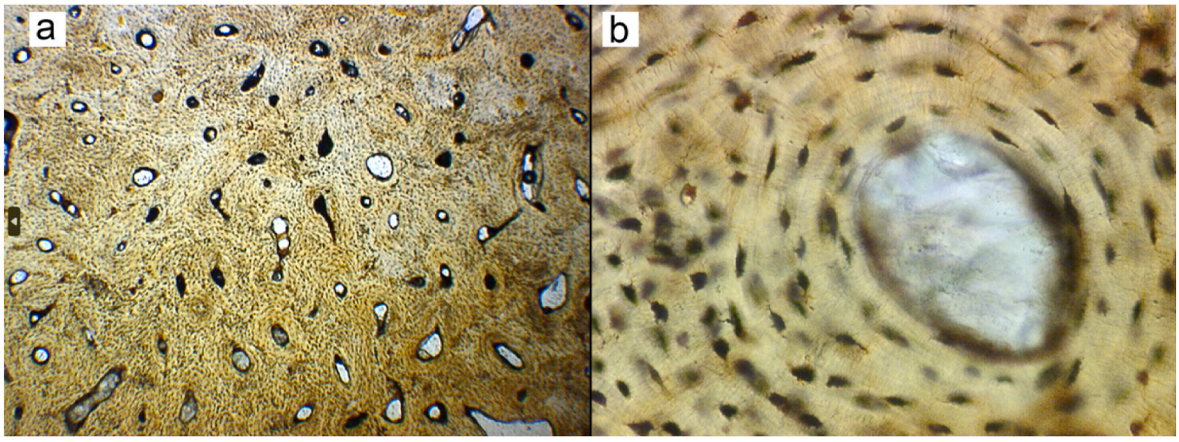

Fig. 7. Higher histological magnification of Fig. 6a, showing the enlargement of Haversian canals of the compact bone: a) cortical bone showing many secondary osteons (40X); b) an enlarged Haversian canal with osteocytes lacunae (400X).

treponemal diseases, the histological features at the periosteal level are represented by characteristic structures called *polsters* and *grenzstreifen* (Schultz, 2001; von Hunnius et al., 2006). These features were not found in Vn-H1, hence eliminating treponemal disease as the origin for this lesion.

4.3.5. Traumas

Traumatic events can directly affect bone, causing a fracture, or affect the soft tissues causing an injury or a hematoma. A hemorrhagic process can occur on the external bone surface in both cases. The periosteal reaction produces a layer or multiple layers of newly built bone; microscopically, changes are represented by short bone trabeculae showing extensive bridging; the original bone substance is unaffected (Cappella and Cattaneo, 2019).

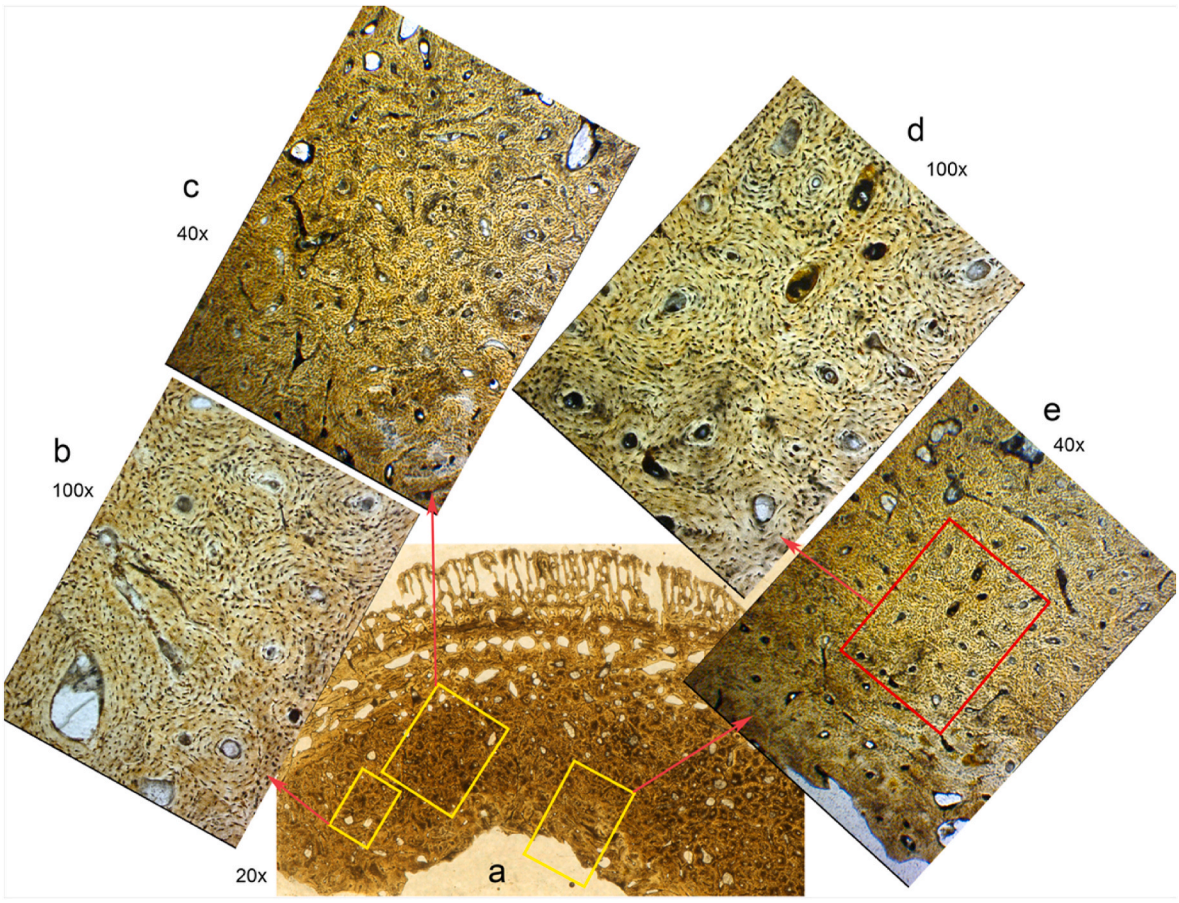

Fig. 8. Histological magnifications at the light microscope of the thin-section of the diaphysis show the compact bone (b,c) and endosteum (d,e).

4.3.6. *Scurvy*

This metabolic disease is caused by a severe vitamin C deficiency resulting in impaired collagen synthesis and inducing subperiosteal hemorrhage. Such as in traumas, the hemorrhagic process stimulates the periosteal reaction and new bone formation. In scurvy, periosteal alteration usually affects the cranial bones and the extremities of long bones, specifically in cases of juvenile scurvy in infants (Geber and Murphy, 2012). Differently from Vn-H1, the histological features of a hemorrhagic condition, such as that caused by trauma or scurvy, are only found external to the original bone surface (Schulz, 2011).

4.3.7. *Hypervitaminosis A*

The excessive intake of vitamin A leads to this metabolic disorder, resulting in a compact periosteal reaction that affects the long bones' midshaft. High intakes of organ meat (specifically liver) in a diet can cause hypervitaminosis A. Changes that result in this condition are found in periosteal and endosteal bone; the new bone formation is essentially sub-periosteal (De Sèze and Ryckewaert, 1979). This pattern of cortical to endosteal remodeling disturbance was not observed in the Vn-H1 specimen the paleopathological record for hypervitaminosis A is infrequent in literature, although a possible lesion observed on a *Homo erectus* femoral bone from Koobi Fora was offered (Walker et al., 1982).

4.3.8. *Other hypotheses*

Other diseases can produce new bone apposition on the shaft surface of the long bones, such as Paget's chronic bone inflammation causing severe bone enlargement and deformities of the bones. In Vn-H1, the histological mosaic pattern pathognomonic of Paget's disease is absent (Ortner, 2003; Grauer and Roberts, 2019). Skeletal fluorosis, due to the ingestion of large amounts of fluoride, induce a periosteal reaction affecting all the skeletons, but unlike Vn-H1, the new bone formation also involves the medullary canal and prevalently results in ossification of the ligaments (Krishnamachari, 1986; Ortner, 2003; Brickley and Mays, 2019). Secondary hypertrophic osteoarthropathy is another disorder causing new bone apposition in the tubular bone, especially in the distal ends of the long bones; it is mainly associated with pulmonary and cardiac diseases and neoplasms (Callemeyn et al., 2016). It typically produces widely distributed periosteal reactions with thick secondary stratified layers not found in Vn-H1.

Histological features of bone remodeling and modeling can help address the differential diagnosis. In Vn-H1. The periosteal reaction consists of an outer layer of woven bone characterized by radiating trabeculae in parallel orientation with bridging (Fig. 6). In the underlying periosteal envelope compact bone, the lamellar bone is disorganized with large circular spaces and enlargement of the Haversian canals (Figs. 6 and 7). This might be the result of hypervascularization related to an inflammatory response. Although osteopenia origins should be ruled out since there is considerable cortical thickness and minimal intra-cortical bone loss. It appears that the histological picture is compatible with a process of inflammatory rather than hemorrhagic or neoplastic origin. Inflammatory origins for bone modeling (the formation of woven bone) include metabolic disorder and or a lack of key nutrients in the diet. These are the most likely origins for this lesion (Weston, 2009, 2012).

Woven bone development along the periosteum is often associated with endochondral bone formation as part of a healing episode. This is initiated by an inflammatory process that starts osteoblastic recruitment and function (Fazzalari, 2011). The time for mesenchymal cells to become osteoblastic cells that can be detected by bone formation is about 4 months (Rutkovskiy et al., 2016). Our lesion is well developed

indicating a bone formation process that is much longer than 4 months, making the case that this lesion is the result of a chronic condition.

4.3.9. Tentative diagnosis

The interpretation of the etiological factors involved in the pathological alteration affecting Vn-H1 has been based on macroscopic and microscopic evaluation. The histopathological investigation revealed features typical of an inflammatory process affecting the bone surface and outer layer. Periosteal reaction is a nonspecific response to a wide variety of diseases. Our conclusion is that a periosteal alteration of inflammatory origin (periostitis) is the more plausible disorder affecting the fossil femur Vn-H1. Unfortunately, it is not possible to be conclusive as at its origins/casual factor: the periosteum responds similarly to the different factors that induce inflammation, and it does not allow us to determine the exact disease etiology for this lesion. Given that the individual had lived with this condition for a while long (*i.e.*, more than the time that the bone needs to remodel, that is more than one week, at least for traumas; Moraitis and Spiliopoulou, 2016, with refences therein), it is likely that the pathological condition was chronic inflammatory process, that affected Vn-H1's life course.

5. Concluding remarks

In this article, we have reported the comparative morphometric analysis of the femoral diaphysis (Vn-H1) discovered in 1985 during systematic excavations in the Paleolithic site of Venosa Notarchirico (southern Italy) that were led by the late Marcello Piperno (*e.g.*, Piperno, 1999). This discovery is implemented by new archaeological and paleontological findings, combined with a grid of absolute dates, obtained in the framework of field activities conducted in the last years on the site under the direction of one of us (MHM).

The most relevant new evidence is the 40Ar/39Ar dating of the femur to an age bracket between 661 and 614 ka (Pereira et al., 2015), which posits Vn-H1 as the oldest hominin fossil found so far in the Italian peninsula (*e.g.*, Buzi et al., 2021) and among the oldest in Europe after MIS 18-16 (Di Vincenzo and Manzi, 2023; Hu et al., 2023). Moreover, the 15 layers of Venosa-Notarchirico, with lithic and faunal remains, represent the most extended sequence of human occupation dated to MIS 17-16, at least in Southern Italy (Moncel et al., 2019, 2020, 2023). This site is, therefore, unique within Europe in showing, at the same time, one of the earliest evidence of an Acheulean lithic assemblage starting from about 680 ka, followed by phases of occupation with or without handaxes. This occurrence must be seen in a scenario where Acheulean sites are not clearly observed in Western Eurasia before 700 ka (*e.g.*, Di Vincenzo and Manzi, 2023; but see Ollé et al., 2023).

Vn-H1 represents the proximal two-thirds of a right femur lacking the proximal epiphyseal region. According to our comparative morphometric analysis, we argue it belonged to an immature individual, possibly a late adolescent, in contrast to the previous attribution to an adult female (Belli et al., 1991). In addition, its features suggest that the specimen may refer to an archaic (*i.e.*, non-modern) human species, without morphological affinities to fossil samples of the Neanderthal lineage. We are therefore inclined to believe that Vn-H1 belonged to *Homo heidelbergensis* (Shoetensack, 1908); as a matter of fact, despite being a controversial species (*e.g.*, Stringer, 2012, 2022), this taxon undoubtedly retains naming priority for specimens with the aforementioned features.

We have also discussed the periosteal alteration that affected Vn-H1, as already reported (Belli et al., 1991). We have described in detail this pathological condition, which is particularly evident in some preserved portions of the mid-shaft. Our analysis was also supported by the histological examination that we have been able to perform on a cross-section of the diaphysis that was obtained in the past, but remained unpublished. Our reappraisal reveals postmortem damage of the cortical surface; at the same time, the surface of the bone has a clear porotic appearance with thin longitudinal striations, confirming the presence of bone neoformation 1–2 mm thick. This evidence is typical of an inflammatory process affecting the bone surface and outer layer. While it's not possible to determine the exact cause of this lesion, we have nonetheless discussed it using a differential diagnosis procedure. We conclude that it was an alteration of inflammatory origin, likely an ongoing process of nonspecific periosteal response that occurred until the death of the individual.

Author contributions

Ileana Micarelli (writing, osteology and paleopathology) Simona Minozzi (writing, histology and paleopathology) Laura Rodriguez (writing, morphology and phylogeny) Fabio di Vincenzo (writing, morphology and phylogeny) Rebeca García-González (writing, morphology and phylogeny) Valentina Giuffra (writing, histology and paleopathology) Robert R. Paine (writing, histology and paleopathology) José-Miguel Carretero (writing, morphology and phylogeny), Gino Fornaciari (writing, histology and paleopathology) Marie-Hélène Moncel (writing, excavation, project management) Giorgio Manzi (writing, conceptualization, coordination).

Declaration of competing interest

The authors declare that they have no known competing financial interests or personal relationships that could have appeared to influence the work reported in this paper.

Data availability

Data will be made available on request.

Acknowledgements

We thank the Soprintendenza A.B.A.P. della Basilicata (Italy) for support and scientific assistance, especially dr. T.E. Cinquantaquattro, dr. F. Canestrini, dr. R. Pirraglia, and dr. S. Mutino. We also thank the Museo Archeologico Nazionale "M. Torelli" di Venosa, the Municipality of Venosa and its Mayor, dr. A. Mantrisi; thedr.ssa Grazia Bulgarelli. Analyses were carried out with the support of the ERC-Adv. LATEUROPE n°101052653, the Leakey Foundation ("Early Evidence of Acheulean bifacial technology in Europe" grant, 2015–2016 and 2019–2021), the National Museum of Natural History, Paris, France (ATM Action Transversale du Muséum, 2016–2018), the Ministerio de Ciencia, Innovación y Universidades, Spain (Grant PID 2021-122355NB-C31 funded by MCIN/AEI/10.13039/501100011033 and "ERDF A way of making Europe"), and the Ministero dell'Istruzione dell'Università e della Ricerca, Italy (PRIN projects 2015: WPHSCJ-LS8 and WPHSCJ).

References

Aiello, L.C., Dean, C., 1990. An Introduction to Human Evolutionary Anatomy. Academic Press Limited, London.

Arsuaga, J.L., Martinez, I., Gracia, A., Carretero, J.M., 1992. Cranial and postcranial remains at the Sima de los Huesos (Sierra de Atapuerca) and human evolution during the Middle Pleistocene. In: Bermudez, J.M., Arsuaga, J.L., Carbonell, E. (Eds.), Human Evolution in Europe and the Atapuerca Evidence. Junta de Castilla y León, Valladolid, pp. 283–304.

Arsuaga, J.L., Martínez, I., Arnold, L.J., Aranburu, A., Gracia-Téllez, A., Sharp, W.D., Quam, R.M., Falguères, C., Pantoja-Pérez, A., Bischoff, J., Poza-Rey, E., Parés, J.M., Carretero, J.M., Demuro, M., Lorenzo, C., Sala, N., Martinón-Torres, M., García, N., Alcázar de Velasco, A., Cuenca-Bescós, G., Gómez-Olivencia, A., Moreno, D., Pablos, A., Shen, C.-C., Rodríguez, L., Ortega, A.I., García, R., Bonmatí, A., Bermúdez de Castro, J.M., Carbonell, E., 2014. Neandertal roots: Cranial and chronological evidence from Sima de los Huesos. Science 344, 1358.

Arsuaga, J.L., Carretero, J.M., Lorenzo, C., Gomez-Olivencia, A., Pablos, A., Rodriguez, L., Garcia-Gonzalez, R., Bonmati, A., Quam, R., Pantoja-Perez, A., Martinez, I., Aranburu, A., Gracia-Tellez, A., Poza-Rey, E., Sala, N., García, N., Alcazar de Velasco, A., Cuenca-Bescós, G., Bermudez de Castro, J.M., Carbonell, E., 2015. Postcranial morphology of the middle Pleistocene humans from Sima de los Huesos, Spain. Proc. Natl. Acad. Sci. USA 112, 11524–11529.

Aufderheide, A.C., Rodríguez-Martin, C., 1998. The Cambridge Encyclopedia of Human Palaeopathology. Cambridge University Press, Cambridge.
Belli, G., Belluomini, G., Segre-Naldini, E., Cassoli, P.F., Cecchi, S., Cucarzi, M., Delitala, L., Fornaciari, G., Mallegni, F., Piperno, M., Segre, A., 1991. Découverte d'un fémur humain acheuléen à Notarchirico (Venosa, Basilicate). L'Anthropologie 95, 47–88.
Bermúdez de Castro, J.M., Martínez, I., Gracia-Téllez, A., Martinón-Torres, M., Arsuaga, J.L., 2021. The Sima de los Huesos Middle Pleistocene hominin site (Burgos, Spain). Estimation of the number of individuals. Anat. Rec. 304 (7), 1463–1477.
Brickley, M.B., Mays, S., 2019. Metabolic disease. In: Buikstra, J. (Ed.), Ortner's Identification of Pathological Conditions in Human Skeletal Remains. Academic Press, pp. 531–566.
Burr, D.B., Allen, M.R. (Eds.), 2014. Basic and Applied Bone Biology. Academic Press, London.
Buzi, C., Di Vincenzo, F., Profico, A., Manzi, G., 2021. The pre-modern human fossil record in Italy from the Middle to the Late Pleistocene: an updated reappraisal. Alpine and Mediterranean Quaternary 34 (1), 17–32.
Callemeyn, J., Van Haecke, P., Peetermans, W.E., Blockmans, D., 2016. Clubbing and hypertrophic osteoarthropathy: insights in diagnosis, pathophysiology, and clinical significance. Acta Clin. Belg. 71 (3), 123–130.
Cappella, A., Cattaneo, C., 2019. Exiting the limbo of perimortem trauma: a brief review of microscopic markers of hemorrhaging and early healing signs in bone. Forensic Sci. Int. 302, 109856.
Carretero, J.M., Lorenzo, C., Arsuaga, J.L., 1999. Axial and appendicular skeleton of Homo antecessor. J. Hum. Evol. 37, 459–499.
Carretero, J.M., Rodríguez, L., García-González, R., Arsuaga, J.L., 2023. Main morphological characteristics and sexual dimorphism of hominin adult femora from the Sima de los Huesos Middle Pleistocene site (Sierra de Atapuerca, Spain). Anat. Rec. 1–31.
Chevalier, T., Lumley, M.-A. de, 2018. Les fémurs Laz 13, Laz 15 et Laz 17, Laz 25 de la grotte du Lazaret. In: Lumley, M.-A. de (Ed.), Les restes humains fossiles de la grotte du Lazaret, Nice, Alpes-Maritimes, France, Des Homo erectus européens évolués en voie de néandertalisation, Chapitre 15. CNRS Éditions, Paris, pp. 435–468.
Chevalier, T., Lumley, M.A. de, 2022a. Lower limb bone structure of Middle Pleistocene hominins from the Caune de l'Arago (Tautavel, France): Evolutionary and functional comparison with the penecontemporaneous hominins of Sima de los Huesos (Atapuerca, Spain). L'anthropologie 126 (4), 103065.
Chevalier, T., Lumley, M.A. de, 2022b. Le membre inférieur de l'Homme de la Caune de l'Arago. Les fémurs de l'Homme de la Caune de l'Arago (A17, A38, A48, A51, A53, A57, A141). In: Lumley, M.-A. de (Ed.), Les restes humains du Pléistocène moyen de la Caune de l'Arago. Caune de l'Arago. Tautavel-en-Roussillon, Pyréné es-Orientales, France, Chapitre, vol. 14. CNRS Éditions, Paris, p. 14.1.
Chevalley, T., Bonjour, J.P., Ferrari, S., Rizzoli, R., 2009. The influence of pubertal timing on bone mass acquisition: a predetermined trajectory detectable five years before menarche. J. Clin. Endocrinol. Metabol. 94, 3424–3431.
Cowgill, L.W., 2010. The ontogeny of Holocene and Late Pleistocene human postcranial strength. Am. J. Phys. Anthropol. 141, 16–37.
Day, M.H., 1971. Postcranial remains of Homo erectus from bed IV, Olduvai Gorge, Tanzania. Nature 232, 383–387.
Lumley, M.A. de, Lamy, P., 1982. Le membre inferieur de l'homme de Tauteval: femurs et fibulae. L'Homo erectus et la Place de l'Homme de Tauteval parmi les Hominidés Fossils. CNRS Éditions, Paris, pp. 276–318.
De Sèze, S., Ryckewaert, A., 1979. Malattie delle ossa e delle articolazioni, p. 2509. Gaggi, Bologna.
Di Vincenzo, F., Manzi, G., 2023. *Homo heidelbergensis* as the Middle Pleistocene common ancestor of Denisovans, Neanderthals and modern humans. Journal of Mediterranean Earth Sciences 15.
Dougherty, R., Kunzelman, K.H., 2007. Computing local thickness of 3D structures with ImageJ. Microsc. Microanal. 13, 1678–1679.
Fazzalari, N.L., 2011. Bone fracture and bone fracture repair. Osteoporos. Int. 22, 2003–2006.
Frisancho, A.R., Garn, S.M., Ascoli, W., 1970. Subperiosteal and endosteal bone apposition during adolescence. Hum. Biol. 639–664.
Frost, H.M., 1985. The "new bone": some anthropological potentials. Am. J. Phys. Anthropol. 28 (S6), 211–226.
García-González, R., Rodriguez, L., Carretero, J.M., Arsuaga, J.L., 2016. The ontogeny of femoral strength in Middle Pleistocene humans from Sima de los Huesos (Atapuerca, Spain). In: Proceedings of the European Society for the Study of Human Evolution. European Society for the Study of Human Evolution, p. 105. Alcalá de Henares, Madrid.
García-González, R., Rodríguez, L., Muñoz-Guarinos, J., Sánchez-Puente, Z., Fernández-Viejo, M., Cirotto, N., Navarro-Pérez, A., García-Barreiro, M., Salazar-Fernández, A., Quintino, Y., Adán-Álvarez, G., Carretero, J.M., 2024. Paleodemographic profiles of the populations buried in san Pablo convent (Burgos. Spain). ENTEMU (UNED-OVIEDO) XX (in press).
Garn, S., 1970. The Earlier Loss and Later Gain of Cortical Bone, vol. 29. CC Thomas, Springfield, IL.
Geber, J., Murphy, E., 2012. Scurvy in the Great Irish Famine: Evidence of vitamin C deficiency from a mid-19th century skeletal population. Am. J. Phys. Anthropol. 148 (4), 512–524.
Geraads, D., Tchernov, E., 1983. Fémurs humains du Pléistocène moyen de Gesher Benot Yaacov (Israël). L'Anthropologie, 87 (1), 138–141.
Gilbert, W.H., 2008. Daka member hominid postcranial remains. In: Gilbert, W.H., Asfaw, B. (Eds.), Homo Erectus, Pleistocene Evidence from Middle Awash, Ethiopia, the Middle Awash Series. University of California Press, pp. 373–396.
Gocha, T.P., Robling, A.G., Stout, S.D., 2018. Histomorphometry of human cortical bone: applications to age estimation. In: Katzenberg, M.A., Grauer, A.L. (Eds.), Biological Anthropology of the Human Skeleton. Wiley, New York, pp. 145–187.
Gosman, J.H., Hubbell, Z.R., Shaw, C.N., Ryan, T.M., 2013. Development of cortical bone geometry in the human femoral and tibial diaphysis. Anat. Rec. 296, 774–787.
Grauer, A.L., 2019. Circulatory, reticuloendothelial, and hematopoietic disorders. In: Buikstra, J. (Ed.), Ortner's Identification of Pathological Conditions in Human Skeletal Remains. Academic Press, pp. 491–529.
Grauer, A.L., Roberts, C.A., 2019. Fungal, viral, multicelled parasitic, and protozoan infections. In: Buikstra, J. (Ed.), Ortner's Identification of Pathological Conditions in Human Skeletal Remains. Academic Press, pp. 441–478.
Heim, J.L., 1976. Les hommes fossiles de la Ferrassie. 1."Le" Gisement, les squelettes adultes (crâne et squelette du tronc). Éditions Masson, Paris.
Hershkovitz, I., May, H., Sarig, R., Pokhojaev, A., Grimaud-Hervé, D., Bruner, E., et al., 2021. A middle pleistocene Homo from Nesher Ramla, Israel. Science 372 (6549), 1424–1428. https://doi.org/10.1126/science.abh3169.
Hildebrand, T., Rüegsegger, P., 1997. A new method for the model-independent assessment of thickness in three-dimensional images. J. Microsc. 185, 67–75.
Hu, W., Hao, Z., Du, P., Di Vincenzo, F., Manzi, G., Cui, J., Fu, Y.X., Pan, Y.H., Li, H., 2023. Genomic inference of a severe human bottleneck during the Early to Middle Pleistocene transition. Science 381 (6661), 979–984.
Kennedy, G.E., 1983. Some aspects of femoral morphology in Homo erectus. J. Hum. Evol. 12, 587–616.
Krishnamachari, K.A., 1986. Skeletal fluorosis in humans: a review of recent progress in the understanding of the disease. Prog. Food Nutr. Sci. 10 (3–4), 279–314.
Lefèvre, D., Raynal, J.P., Vernet, G., Kieffer, G., Piperno, M., 2010. Tephro-stratigraphy and the age of ancient southern Italian Acheulean settlements: the sites of Loreto and Notarchirico (Venosa, Basilicata, Italy). Quat. Int. 223, 360–368.
Mallegni, F., Mariani-Costantini, R., Fornaciari, G., Longo, E.T., Giacobini, G., Radmilli, A.M., 1983. New European fossil hominid material from an Acheulean site near Rome (Castel di Guido). Am. J. Phys. Anthropol. 62, 263–274.
Mallegni, F., Piperno, M., Segre, A., 1987. Human remains of *Homo* sapiens neanderthalensis from the pleistocene deposit of Sants Croce Cave, Bisceglie (Apulia), Italy. Am. J. Phys. Anthropol. 72 (4), 421–429.
Manzi, G., 2011. Before the emergence of Homo sapiens: overview on the Early-to-Middle Pleistocene fossil record (with a proposal about *Homo heidelbergensis* at the subspecific level). Int. J. Evol. Biol. 2011.
Manzi, G., 2016. Humans of the Middle Pleistocene: the controversial calvarium from Ceprano (Italy) and its significance for the origin and variability of *Homo heidelbergensis*. Quat. Int. 411, 254–261.
Manzi, G., Magri, D., Milli, S., Palombo, M.R., Margari, V., Celiberti, V., Barbieri, Mar, Barbieri, Mau, Melis, R.T., Rubini, M., Ruffo, M., Saracino, B., Tzedakis, P.C., Zarattini, A., Biddittu, I., 2010. The new chronology of the Ceprano calvarium (Italy). J. Hum. Evol. 59, 580–585.
Marques, C., 2019. Tumors of bone. In: Buikstra, J. (Ed.), Ortner's Identification of Pathological Conditions in Human Skeletal Remains. Academic Press, Cambridge, pp. 639–717.
Martin, R, Saller, K, 1957. Lehrbuch der Anthropoogie. Stuttgart Gustav Fischer.
Materialise, N., 2009. Mimics, 13 ed www.materialise.be.
McCown, T.D., Keith, A., 1939. The Stone Age of Mount Carmel II: the Fossil Human Remains from the Levalloiso-Mousterian. Clarendon Press, Oxford.
McFarlin, S.C., Terranova, C.J., Zihlman, A.L., Bromage, T.G., 2016. Primary bone microanatomy records developmental aspects of life history in catarrhine primates. J. Hum. Evol. 92, 60–79.
Moncel, M.H., Santagata, C., Pereira, A., Nomade, S., Bahain, J.-J., Voinchet, P., Piperno, M., 2019. Biface production at Notarchirico (Southern Italy) before 600 ka? Contribution to the earliest evidence of the European Acheuleans. PLoS One 14 (9), e0218591.
Moncel, M.H., Santagata, C., Pereira, A., Nomade, S., Voinchet, P., Bahain, J.-J., Daujeard, C., Curci, A., Lemorini, C., Hardy, B., Eramo, G., Berto, C., Raynal, J.-P., Arzarello, M., Mecozzi, B., Iannucci, A., Sardella, R., Allegretta, I., Delluniversità, E., Terzano, R., Dugas, P., Jouanic, G., Queffelec, A., d'Andrea, A., Valentini, R., Minucci, E., Carpentiero, L., Piperno, M., 2020. The origin of early Acheulean expansion in Europe 700 ka ago: new findings at Notarchirico (Italy). Sci. Rep. 10 (1), 1–16.
Moncel, M.H., Lemorini, C., Eramo, G., Fioretti, G., Daujeard, C., Curci, A., Berto, C., Hardy, B., Pineda, A., Rineau, V., Carpentieri, M., Sala, B., Arzarello, M., Mecozzi, B., Iannucci, A., Sardella, R., Piperno, M., Piperno, M., 2023. A taphonomic and spatial distribution study of the new levels of the middle Pleistocene site of Notarchirico (670–695 ka, Venosa, Basilicata, Italy). Archaeological and Anthropological Sciences 15 (7), 106.
Moraitis, K., Spiliopoulou, C., 2016. Identification and differential diagnosis of perimortem blunt force trauma in tubular long bones. Forensic Sci. Med. Pathol. 2 (4), 221–229.
Moreno, D., Falguères, C., Pérez-González, A., Voinchet, P., Ghaleb, B., Despriée, J., Bahain, J.-J., Sala, R., Carbonell, E., Bermúdez de Castro, J.M., Arsuaga, J.L., 2015. New radiometric dates on the lowest stratigraphical section (TD1 to TD6) of Gran Dolina site (Atapuerca, Spain). Quat. Geochronol. 30, 535–540.
Ollé, A., Lombao, D., Asryan, L., García-Medrano, P., Arroyo, A., Fernández-Marchena, J. L., Vallverdú, J., 2023. The earliest European Acheulean: new insights into the large shaped tools from the late Early Pleistocene site of Barranc de la Boella (Tarragona, Spain). Front. Earth Sci. 11, 1188663.
Ortner, D.J., 2003. Identification of Pathological Conditions in Human Skeletal Remains, vol. 543. Academic Press, Cambridge.
Parfitt, A.M., Drezner, M.K., Glorieux, F.H., Kanis, J.A., Malluche, H., Meunier, P.J., Ott, S.M., Recker, R.R., 1987. Bone histomorphometry: standardization of

nomenclature, symbols, and units: report of the ASBMR Histomorphometry Nomenclature Committee. J. Bone Miner. Res. 2 (6), 595–610.
Pereira, A., Nomade, S., Voinchet, P., Bahain, J.J., Falguères, C., Garon, H., Lefèvre, D., Raynal, J.P., Scao, V., Piperno, M., 2015. The earliest securely dated hominin fossil in Italy and evidence of Acheulian occupation during glacial MIS 16 at Notarchirico (Venosa, Basilicata, Italy). J. Quat. Sci. 30, 639–650.
Piperno, M., 1999. Notarchirico. Un sito del Pleistocene medio iniziale nel bacino di Venosa. Osanna Edizioni, Venosa.
Puymerail, L., Ruff, C.B., Bondioli, L., Widianto, H., Trinkaus, E., Macchiarelli, R., 2012. Structural analysis of the Kresna 11 Homo erectus femoral shaft (Sangiran, Java). J. Hum. Evol. 63, 741–749.
Rana, R.S., Wu, J.S., Eisenberg, R.L., 2009. Periosteal reaction. Am. J. Roentgenol. 193 (4), W259–W272.
Raynal, J.-P., Lefèvre, D., Vernet, G., Papy, G., 1999. Un bassin, un volcan: lithostratigraphie du site acheuleen de Notarchirico (Venosa, Basilicate, Italia). In: Piperno, M. (Ed.), *Notarchirico; Un sito del Pleistocene medio- antico nel bacino di Venosa (Basilicata)*, Osanna. Museo Nazionale Preistorico Etnografico "L. Pigorini, Roma, pp. 175–205.
Rineau, V., Moncel, M.H., Zeitoun, V., 2022. Revealing evolutionary patterns behind homogeneity: the case of the Palaeolithic assemblages from Notarchirico (Southern Italy). J. Archaeol. Method Theor 30 (1), 203–238.
Roberts, C.A., 2019. Infectious disease: introduction, periostosis, periostitis, osteomyelitis, and septic arthritis. In: Buikstra, J. (Ed.), Ortner's Identification of Pathological Conditions in Human Skeletal Remains. Academic Press, pp. 285–319.
Robling, A.G., Stout, S.D., 1999. Morphology of the drifting osteon. Cells Tissues Organs 164 (4), 192–204.
Rodriguez, L., 2013. Estudio biomecánico de los huesos largos del esqueleto apendicular de los homínidos del Pleistoceno Medio de la Sima de los Huesos. *Sierra de Atapuerca (Burgos): Implicaciones paleobiológicas y filogenéticas* (Doctoral). Universidad de Burgos, Burgos.
Rodríguez, L., Carretero, J.M., García-González, R., Arsuaga, J.L., 2018. Cross-sectional properties of the lower limb long bones in the Middle Pleistocene Sima de los Huesos sample (Sierra de Atapuerca, Spain). J. Hum. Evol. 117, 1–12.
Ruff, C.B., Hayes, W.C., 1983. Cross-sectional geometry of Pecos Pueblo femora and tibiae—a biomechanical investigation: I. Method and general patterns of variation. Am. J. Phys. Anthropol. 60, 359–381.
Ruff, C.B., Trinkaus, E., Walker, A., Spencer-Larsen, C., 1993. Postcranial robusticity in Homo I: temporal trends and mechanical interpretation. Am. J. Phys. Anthropol. 91, 21–53.
Ruff, C., Puymerail, L., Macchiarelli, R., Sipla, J., Ciochon, R.L., 2015. Structure and composition of the Trinil femora: functional and taxonomic implications. J. Hum. Evol. 80, 147–158.
Ruff, C.B., Sylvester, A.D., Rahmawati, N.T., Suriyanto, R.A., Storm, P., Aubert, M., Berghuis, H., Pop, E., Batenburg, K.J., Coban, S.B., Kostenko, A., Noerwidi, S., Renema, W., Adhityatama, S., Joordens, J., 2022. Two late pleistocene human femora from Trinil, Indonesia: implications for body size and behavior in southeast Asia. J. Hum. Evol. 172, 103252.
Rutkovskiy, A., Stensløkken, K.O., Vaage, 2016. Osteoblast Differentiation at a Glance. Medical Science Monitor Basic Research 22, 95–106.
Santagata, C., Moncel, M.H., Piperno, M., 2020. Bifaces or not bifaces? Role of traditions and raw materials in the Middle Pleistocene. The example of levels E-E1, B and F (610-670 ka) at Notarchirico (Italy). Journal of Archaeological Sciences. Reports 33, 102544.
Schultz, M., 2001. Paleohistopathology of bone: a new approach to the study of ancient diseases. Yearbk. Phys. Anthropol. 44, 106–147.
Schultz, M., 2011. Light microscopic analysis of macerated pathologically changed bones. In: Crowder, C., Stout, S. (Eds.), Bone Histology. CRC Press, Boca Raton, pp. 269–312.
Shoetensack, O., 1908. Der Unterkiefer des *Homo Heidelbergensis* aus den Sanden von Mauer bei Heidelberg. Ein Beitrag zur Paläontologie des Menschen. Zur Vererbungslehre 1, 408–410.
Stout, S.D., Paine, R.R., 1992. Histological age estimation using rib and clavicle. Am. J. Phys. Anthropol. 87 (1), 111–115.
Stringer, C.B., 2012. The status of *Homo heidelbergensis*, Schoetensack 1908. Evol. Anthropol. 21, 101–107.
Stringer, C.B., 2022. The development of ideas about a recent African origin for *Homo sapiens*. Journal of Anthropological Sciences 100, 5–18.
Swan, K.R., Ives, R., Wilson, L.A., Humphrey, L.T., 2020. Ontogenetic changes in femoral cross-sectional geometry during childhood locomotor development. Am. J. Phys. Anthropol. 173, 80–95.
Tillier, A.M., 2005. The Tabun C1 skeleton: a levantine neanderthal? Mitekufat Haeven: Journal of the Israel Prehistoric Society/439–450 מתקופת האבן.
Trinkaus, E., 1983. The Shanidar Neandertals. Academic Press, New York.
Trinkaus, E., 2016. The Krapina Human Postcranial Remains: Morphology, Morphometrics and Paleopathology. Faculty of Humanities and Social Sciences, University of Zagreb.
Trinkaus, E., Ruff, C.B., 1999. Diaphyseal cross-sectional geometry of near Eastern middle Palaeolithic humans: the femur. J. Archaeol. Sci. 26, 409–424.
Trinkaus, E., Ruff, C.B., 2012. Femoral and tibial diaphyseal cross-sectional geometry in pleistocene Homo. PaleoAnthropology 13–62.
Trinkaus, E., Ruff, C.B., Churchill, S.E., Vandermeersch, B., 1998. Locomotion and Body Proportions of the Saint-Césaire 1 Châtelperronian Neandertal, vol. 95. Proceedings of the National Academy of Sciences, pp. 5836–5840.
Vallverdú, J., Saladié, P., Rosas, A., Huguet, R., Cáceres, I., Mosquera, M., Garcia-Tabernero, A., Estalrrich, A., Lozano-Fernández, I., Pineda-Alcalá, A., Carrancho, Á., Villalaín, J.J., Bourlès, D., Braucher, R., Lebatard, A., Vilalta, J., Esteban-Nadal, M., Bennàsar, M.L., Bastir, M., López-Polín, L., Ollé, A., Vergés, J.M., Ros-Montoya, S., Martínez-Navarro, B., García, A., Martinell, J., Expósito, I., Burjachs, F., Agustí, J., Carbonell, E., 2014. Age and Date for Early Arrival of the Acheulian in Europe (Barranc de la Boella, la Canonja, Spain). PLoS One 9, e103634.
von Hunnius, T.E., Roberts, C.A., Boylston, A., Saunders, S.R., 2006. Histological identification of syphilis in pre-Columbian England. Am. J. Phys. Anthropol. 129, 559–566.
Wagner, G.A., Krbetschek, M., Degering, D., Bahain, J.J., Shao, Q., Falguères, C., Voinchet, P., Dolo, J., Garcia, T., Rightmire, G.P., 2010. Radiometric dating of the type-site for Homo heidelbergensis at Mauer, Germany. Proceedings of the National Academy of Sciences USA 107, 19726–19730.
Waldron, T., 2009. Palaeopathology. Cambridge University Press, Cambridge.
Walker, A., Zimmerman, M.R., Leaky, R.E.F., 1982. A possible case of hypervitaminosis A in *Homo erectus*. *Nature*, 296, 248–250.
Weidenreich, F., 1941. The extremity bones of Sinanthropus pekinensis. Paleontologia Sinica 5, 373–383.
Weston, D.A., 2009. Brief communication: paleohistopathological analysis of pathology museum specimens: can periosteal reaction microstructure explain lesion etiology? Am. J. Phys. Anthropol. 140 (1), 186–193.
Weston, D.A., 2012. Nonspecific infection in paleopathology: interpreting periosteal reactions. In: Grauer, A.L. (Ed.), A Companion to Paleopathology. Blackwell Publishing Ltd., Chichester, pp. 492–512.